4-9-2019

Starved Lubrication using Ionic Liquid as an Additive to Biodegradable Oil in Titanium-Ceramic Contact

Sameer Magar
sam7088@rit.edu

ROCHESTER INSTITUTE OF TECHNOLOGY

Starved Lubrication using Ionic Liquid as an Additive to Biodegradable Oil in Titanium-Ceramic Contact

Submitted by,

Sameer Magar

A Thesis Submitted in Partial Fulfillment of the Requirement for Master of Science in Mechanical Engineering

Department of Mechanical Engineering

Kate Gleason College of Engineering

Approved by:

Dr. Patricia Iglesias Victoria ----------

Department of Mechanical Engineering **(Advisor)**

Dr. Alfonso Fuentes Aznar ----------

Department of Mechanical Engineering **(Committee Member)**

Dr. Rui Liu ----------

Department of Mechanical Engineering **(Committee Member)**

Dr. Stephen Boedo ----------

Department of Mechanical Engineering **(Department Representative)**

Rochester Institute of Technology

Rochester, New York

04/09/2019

ABSTRACT

Friction leads to energy loss in any system that has two bodies in contact and relative motion with each other. Advancements in lubricants and the lubrication process have helped to reduce friction and in return reduced energy losses owing to friction. But, however, lubricant starvation is still a reality and can happen in applications like piston-ring and cylinder liner contact, and machining etc. It can cause equipment damage leading to unexpected downtime. Ionic liquids, in the recent years have shown a great potential in terms of friction and wear reduction. Using ionic liquids as additives helps reduce the cost of the lubricant considering the high cost of ionic liquids. Mineral oil based lubricant have been very commonly used as the base lubricant. However, they have caused environmental concerns due to the presence of petroleum-based products. The use of biodegradable oil as the base lubricant has proven to be a great alternative. The advancements in composite materials have made the range of materials that we use today more versatile. However, the potential of some monolithic metals like titanium remains unexplored. The major reason for the limited application of titanium is not the limited availability of the metal, but the high cost of machining titanium itself. Ceramic tools are the most commonly used in titanium machining. This study focusses on using an ionic liquid as an additive to a biodegradable oil in starved lubrication regime in titanium-ceramic contact at 3 different frequencies under different loads. Tests were conducted using a reciprocating tribometer with a tungsten carbide ball in contact with the titanium disk. Tests were performed at frequencies of 3Hz, 4Hz and 5Hz. The results showed a maximum 50% reduction in friction coefficient and 23% wear reduction at a frequency of 5 Hz under a load of 2N by using the ionic liquid as an additive to biodegradable oil as compared to using the biodegradable oil as the base lubricant. A maximum wear reduction of

28% was achieved at frequency of 5 Hz under a load of 3N. Moreover, the use of 1% wt. ionic liquid as an additive delayed the spike in friction coefficient by almost 40% as compared to using biodegradable oil as base lubricant. Scanning Electron Microscope analysis showed fewer abrasion marks on the wear track achieved by using 1% wt. protic ionic as additive to biodegradable oil as compared to using biodegradable oil as base lubricant. Energy Dispersive X-ray Spectroscope (EDS) results showed higher amount of carbon inside the wear track when the ionic liquid was present in the lubricant, that proved the presence of a tribolayer.

ACKNOWLEDGEMENT

I would sincerely like to thank Dr. Patricia Iglesias Victoria for all the support and valuable guidance throughout the entire process. I am both grateful and obliged to her for giving me this wonderful opportunity and always believing in me. Her trust and confidence in me always pushed me to be the best version of myself throughout this wonderful journey.

I would also like to thank my thesis committee members Dr. Alfonso Fuentes Aznar, Dr. Rui Liu and Dr. Michael Schrlau for evaluating my work. I would also like to thank my fellow lab-mates Hong Guo, Akshay Gaikwad, Paarth Mehta and Irene Del Sol for all their support and good times in the lab.

Finally, I would also like to thank my parents for supporting and believing in me throughout this journey.

Contents

LIST OF FIGURES

LIST OF TABLES

NOMENCLATURE

[THTDP][Phos] – Trihexyl(tetradecyl)phosphonium bis(2,4,4-trimethylpentyl) phosphinate

DCi - Tri-[bis(2-hydroxyethylammonium)] Citrate

Hz – Hertz

N – Newton

GPa – Giga Pascal

ABBREVIATIONS

IL – Ionic Liquid

MO – Mineral Oil

BO – Biodegradable oil

TiN – Titanium Nitride

TiC – Titanium Carbide

CVD – Chemical Vapor Deposition

CBN – Cubic Boron Nitride

PCD – Polycrystalline Cubic Diamond

MQL – Minimum Quantity Lubrication

SEM – Scanning Electron Microscope

1.0 PROBLEM INTRODUCTION

Friction is a phenomenon that helps us in performing basics tasks in everyday life, like walking and stopping a car. Similarly, without wear we can't even use a pencil or chalk for writing. However, both friction and wear are not desirable in applications like mechanical machines, bearings, seals etc. Friction causes loss of energy and wear of material between the surfaces in contact. Therefore, we use lubrication to reduce friction and wear in sliding and rolling contacts. Another phenomenon called lubrication starvation can lead to equipment damage [1]. Lubrication starvation can be very commonly found in piston-rings to cylinder liner contact as well as in operations like machining.

Considering the application of lubricant in machining; recently Minimum Quantity Lubricant (MQL) has emerged as a new method of using lubricant. Using this method, the lubricant reaches the tool/chip interface through capillarity and forms a thin film at the interface. Multiple studies show that conventional cutting fluid lubricant in MQL is not sufficient to reduce the friction and the associated effects [2]. The application of this method is a perfect example of starved lubrication, where a limited amount of lubricant is provided at the point of contact between the mating surfaces.

Ionic liquids (ILs) have emerged as novel functional fluids that can be used as either lubricants or additives to lubricants [3–6]. ILs are salts in the liquid state whose melting point is below 100°C and are made up of ions with some unique characteristics such as low vapor-pressure, high polarity, high thermal stability, nonflammability, miscibility with water and other organic solvents [7,8]. Halogen-free IL can be used to avoid the harmful elements such as [BF_4] and [PF_6] which can form Hydrogen Fluoride (HF) which is highly corrosive [9]. Ionic Liquid as an

additive to the lubricant using MQL method has shown incredible results at room temperature as well as at 100°C [9–14].

Mineral oils have been used as neat lubricants for a long time. But, however, mineral oils are petroleum-based oils obtained as a product of distillation of crude oil. Therefore, disposing of mineral oils can cause pollution and environmental hazards. The pollution prevention laws are becoming stricter day-by-day and there is a need to find an alternative to mineral oils. One such alternative is the usage of bio-degradable oils as they have high lubricity, high viscosity index, high flash point and low evaporative losses as compared to mineral oils [15].

Titanium and its alloys have excellent material properties such as high strength to weight ratio, good temperature and corrosion resistance, low density and high load-bearing capacity [16]. Owing to these excellent material properties it is ideal for applications in the aerospace industry, rocket production, and shipbuilding. Moreover, titanium has also shown its potential in the automotive, civil and medical industry. However, its use in these industries is limited due to its high cost of manufacturing particularly due to its difficulty to cut.

Machining of titanium and titanium alloys has always been a challenge because of its thermo-mechanical properties. The material properties like low thermal conductivity, high strength and hardness and low Volume specific heat result in high cutting temperatures during machining [2,16]. This increased temperature accelerates high tool wear and early tool failure during machining and ultimately ends up increasing the cost of production. The mostly commonly used tools for machining of titanium are ceramic tools.

2.0 THE RESEARCH QUESTION

The application of biodegradable oil has shown a lot of potential in terms of friction and wear reduction. Various lubricants have been used but, studies show that there is a need for an additive to the conventional lubricants. The aim of this thesis is to understand the friction and wear behavior of titanium-ceramic contact using a halogen-free IL as an additive to a biodegradable oil. The research questions that must be answered are:

- Can the addition of halogen-free Ionic Liquid to a biodegradable oil reduce the friction and wear in titanium-ceramic contact?
- What testing parameters will provide the best reduction in friction and wear?

3.0 LITERATURE REVIEW

3.1 Friction

The term “Tribology” is derived from the Greek word “tribo” which means rubbing and can be defined as the science and technology of interacting surfaces in relative motion [1]. It includes the study of friction, lubrication and wear.

Whenever two bodies are in contact and have relative motion with each other, a resistant force that opposes the relative motion is called as friction [17]. In some components such as car brakes and clutches, friction is of utmost importance. It is also very necessary for everyday life movements such as walking. But friction should be kept as low as possible in most of the cases such as bearings, gears, piston rings etc. In order to save the loss of energy owing to friction, it can be minimized by lubricating the bodies in contact.

3.2 Wear

Wear can be defined as the material removal process from one or both the bodies in contact and having sliding, rolling, impact motion to one another [17]. This is the result of the interaction between these two surfaces in relative motion. During the wear process material can may be removed from one surface and either can be transferred to the mating surface or it may break loose as a wear particle. In case of material transfer from one surface to another, the net Volume or mass loss of the interface is zero, even if one of the surfaces is worn. The definition of wear usually is based on the loss of material, but it should be considered that damage due to material displacement even without any net change in Volume or mass, also constitutes for wear [17].

Depending on the interaction between the two mating surfaces, the type of wear can be categorized in 4 different wear mechanisms as follows:

1. **Adhesive Wear:** In a very small fraction of contact, material can break out of either of the mating surfaces, and a small fragment can get attached to the other surface because of adhesion. Further sliding causes more material to break out. Now these broken out material fragments can get transferred to the mating surface or to another previously attached fragment and thus making the damage even worse [17]. Figure 1 shown the SEM image of cross section of 302 stainless steel in contact with copper plate.

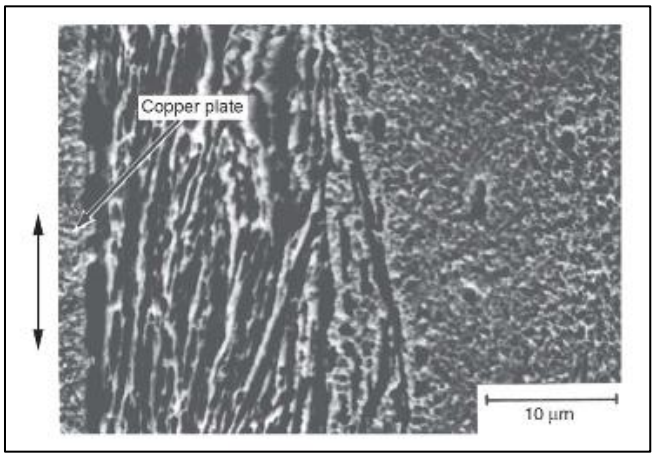

Figure 1: SEM micrograph of cross section of 302 stainless steel in contact with copper plate after adhesive wear. Sliding direction is along the vertical axis [17].

2. **Abrasive Wear:** Abrasive wear usually occurs when the asperities of a rough and hard surface slide on a soft surface resulting in damaging the interface by plastic deformation or fracture [17]. Apart from this there are two more general situations resulting in abrasive wear. The first one is when a hard surface is mounted to a less hard surface like in mechanical operations like grinding and cutting. The second situation is when hard particles from third body come in between two mating surfaces [17]. Figure 2 shows all the situations in which we can see abrasive wear.

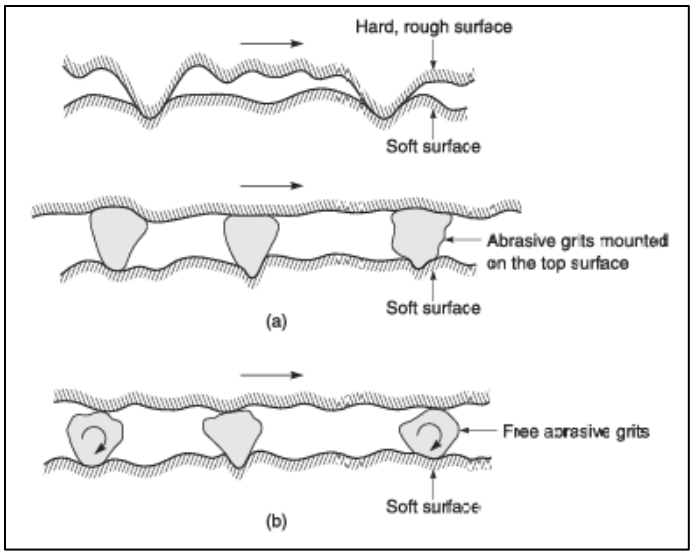

Figure 2: Schematics showing general abrasive wear, (a) a rough hard surface mounted on a surface, and (b) free abrasive grits from a third party caught between two surfaces [17].

3. **Fatigue Wear:** Whenever we have a repeated rolling or sliding action, subsurface and surface fatigues are observed. This means that due to the repeated loading and unloading cycles during the period of motion, formation of surface or subsurface cracks is induced. After a critical number of cycles, this may result in the formation of large fragments, leaving large pits on the surface, also known as pitting [17].
4. **Chemical (Corrosion) Wear:** This type of wear occurs when sliding of the two-mating surface take place in a corrosive environment. Corrosion can occur due to the chemical or electrochemical interaction of the interface with the environment. High temperature and high humidity environments are ideal for chemical corrosion to take place [17].

Finally, the effect of both wear and friction can be limited by the usage of lubrication.

3.3 Lubrication

The sliding motion between clean solid surfaces in contact is characterized by a high coefficient of friction and wear due to properties of the surfaces in contact like low hardness, high surface energy and reactivity. Traces of foreign substances, such as organic compounds are readily adsorbed by the clean surfaces from the environment. After the adsorption process the newly formed surfaces generally have a lower friction coefficient and wear as compared to the clean surface. But, during the sliding process, the presence of a layer of foreign material is not guaranteed. Therefore, lubricants are applied deliberately to produce this layer between the sliding surfaces resulting in low friction and wear. The process of application of lubricant is called as lubrication [17]. Depending on the operating conditions different types of lubrication regimes exist. According to the Stribeck curve as shown in figure 1, the lubrication regimes can be divided into three groups:

- Boundary lubrication: In this regime, the surfaces are in contact and the load is carried by the surface asperities [1].
- Mixed lubrication: In this regime, the load is carried by both the lubricant film and the asperities in contact [1].
- Hydrodynamic lubrication: In this regime, the surfaces are not in contact and a full film of lubricant which is usually thicker than 1 μm, carries the load. Conformal contacts operate in this regime. Hydrodynamic lubrication also includes the elasto-hydrodynamic lubrication regime in which the external load and pressure developed in the film are high enough to consider the elastic deformation of the surfaces [1].

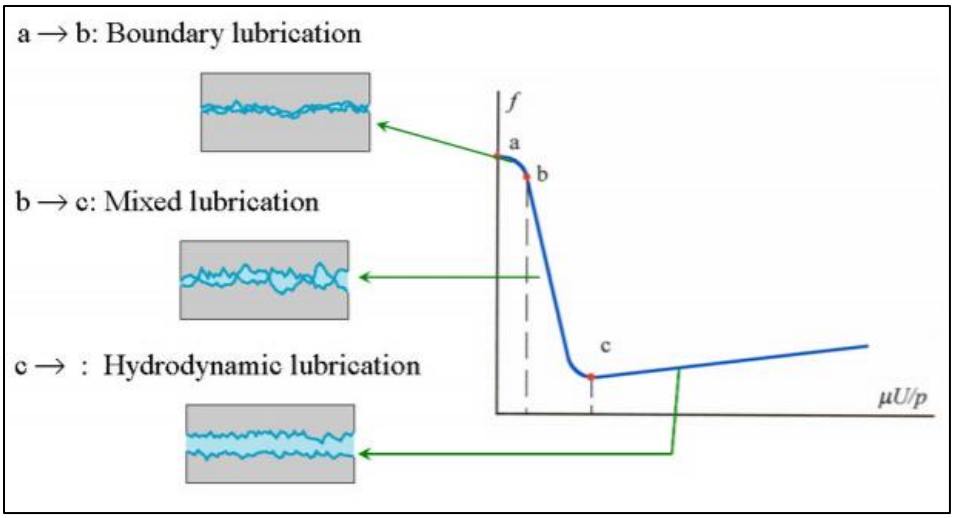

Figure 3: Stribeck curve representing the different lubrication regimes [1]

Figure 1. shows the Stribeck curve which presents the coefficient of friction (f) as a function of the product of absolute viscosity (μ) and rotational speed in revolutions per second (U) divided by the load (p).

These lubrication regimes can be explained in detail as follows:

1. **Boundary Lubrication:** In this regime, the surfaces are in contact and the load is carried by the surface asperities. As can be seen in figure 1, as the load increases, speed or the fluid viscosity decreases and can result in sharp increase in coefficient of friction. This condition can also occur in starved contact. As mentioned earlier it is that condition in which the solid asperities are so close to each other that the surface interaction between monomolecular or multimolecular film of lubricants and the solid asperities dominate the contact. Before the formation of a fluid film due to hydrodynamic lubrication, the contact interfaces operate in the boundary lubrication regime [17].

2. **Mixed Lubrication:** The area between the transition from the boundary lubrication to the hydrodynamic lubrication is known as mixed lubrication in which two lubrication mechanism may

be functioning. This mixed regime is also sometimes referred to as quasi-hydrodynamic, partial fluid, or thin film lubrication [17].

3. **Hydrodynamic Lubrication:** Sometimes, it is also called as fluid-film or thick-film lubrication. Whenever a bearing with convergent shape in the direction of motion starts to move from rest in the longitudinal direction, a thin layer of fluid is pulled due viscous force and then it is compressed between the bearing surfaces. This results in creating enough pressure to support the load without the need of any external pumping source. Hydrodynamic journal and thrust bearings can achieve a high load capacity at high velocities using high viscosity fluids. These bearings are also called as self-acting bearings [17].

3.3.1 Starved Lubrication

As the name suggests, starved lubrication is a regime which is a result of lubricant starvation. Several factors like restricted oil supply, inlet flow design, dry starts, low oil level in sumps, oil foaming, wrong viscosity, worn or improperly operating circulating pumps can lead to lubrication starvation. To avoid lubrication starvation, maintaining a constant and sufficient level of lubrication is required. Whenever lubrication starvation occurs, the fluid film is no longer able to maintain a full separation of moving contacts, which can lead to excessive heat resulting from increased friction, increased wear, noise and vibration and ultimately lead to seizing of the moving mechanical parts [18]. This can cause equipment damage and unplanned downtime in mechanical machines [18].

3.4 Ionic Liquids

As mentioned earlier, ILs are salts with a melting point below 100°C. ILs have impressive physical properties that have made them so successful as lubricants and lubricant additives. These properties such as negligible vapor pressure, high thermal, chemical and electrical stability, non-inflammability and low environmental impact make them ideal for using as lubricants or lubricant additives [19,20].

Low vapor pressure implies that ILs are non-volatile. It also helps in mitigating health, safety and environmental risks. Higher thermal stability implies that ILs can be used across a larger range of operating temperatures. The thermogravimetric analysis proves the thermal stability of ILs.

3.4.1 Halogen-Free Ionic Liquids

The most commonly used ILs in tribology have imidazolium, ammonium and phosphonium as cations and tetrafluoroborates (BF_4) and hexafluorophosphates (PF_6) as anions [19,20]. But, PF_6 and BF_4 and other halogen containing anions absorb water by hydration when they are exposed to moisture resulting in hazardous by-products such as Hydrogen Fluoride (HF) that cause tribocorrosion resulting in increased friction and wear [9]. Hence, halogen-free ionic liquids prevent the formation of hazardous by-products such as HF and thus are a better option than using halogen-containing ILs.

3.4.2 ILs as Neat Lubricants

ILs can be used as lubrication oils as they exhibit good tribological performance in general engineering sliding pairs such as steel-steel, ceramic-ceramic, steel-aluminum etc. Ye et al [3] performed tribological tests to compare the performance of C_2C_6 Imidazolium tetrafluoroborate ($[C_2C_6im]BF_4$) IL with Perfluoropolyether (PFPE) synthetic oil. At a load of 200 N with steel-steel

contact a friction reduction of 50% was achieved using ($[C_2C_6im]BF_4$) as lubricant oil as compared to PFPE. Jiménez and Bermúdez [8] studied the tribological performance of C_1C_6 Imidazolium tetrafluoroborate ($[C_1C_6im]BF_4$) and C_1C_8 Imidazolium tetrafluoroborate ($[C_1C_8im]BF_4$) compared to propylene glycol dioleate (PGDO) under a variety of temperatures at 30°C, 100°C and 200°C. At all three temperatures ILs showed lower friction coefficients for the aluminum-steel contact.

Jiménez and Bermúdez [14] compared the performance of two ILs 1-octyl,3-methylimidazolium tetrafluoroborate (L108) and 1-hexyl,3-methylimidazolium hexafluorophosphate (LP106) with MO. The results showed an impressive 60% friction reduction using L108 as compared to MO and 52% wear reduction using LP106 as compared to MO.

3.4.3 ILs as Additives in Lubricants

Using ILs as neat lubricants can be costly due to the high cost of ILs. Therefore, ILs can be used as an additive to the lubricant. A lot of studies have shown the potential of ILs as additives to lubricants. Bossung, DeRosa, Salas and Iglesias [21] compared the performance of Trihexyltetradecylphosphonium decanoate (Deca) and Trihexyltetradecylphosphonium amide (Tf_2N) as an additive with 1 and 2.5 wt.% to coffee bean oil as lubricant. An impressive 23% and 16% friction reduction was achieved using 1% Deca and 2.5% Tf_2N respectively. Moreover, 21% and 7% wear reduction using 1% Deca and 2.5% Tf_2N respectively was also achieved.

Cigno et al. [4] achieved a wear reduction of 74.3% using halogen-free Trihexyl(tetradecyl) phosphonium [THTDP][Phos] as an additive to base oil in steel-steel contact.

3.4.4 Protic Ionic Liquids

Protic ionic liquids (PILs) are a subset of ILs, which are formed through the combination of Brønsted acid and Brønsted base [22]. Halogen-free protic ionic liquids have been found to be more environment friendly than aprotic ionic liquids (APILs) and they could also be biocompatible [22]. PILs possess a very wide range of properties such as high thermal and electrical conductivity, lower melting point, low-toxicity and non-flammability [22,23]. PILs can be a suitable alternative to APILs due to the ease of synthesis and cheaper cost. Moreover, many acid-base combinations can be used to prepare new PILs. PILs can also be halogen-free that do not contain Fluorine (or any other halogen element), which avoids the formation of HF.

3.4.5 Minimum Quantity Lubrication using Ionic Liquid as an additive to lubricant

Application of cutting fluid using MQL has helped to reduce the temperature in the machining zone as the lubricant reaches the tool-chip interface [2], but the conventional lubricant used in MQL is not effective enough to reduce the friction and associated effects [2]. To achieve improved performance, the base fluid is often coupled with various additives. Nano- particle have found great success by being the required additive [13], but unfortunately their application is still limited by environmental concerns as well as cost. ILs have shown great potential to reduce friction in recent years. Reductions of 60% and 99.5% were noted in friction coefficient and wear rate respectively in titanium-steel sliding contact using 1-octyl-3-methylimidazolium tetrafluoroborate when compared to neat mineral oil [13].

Jayal et al. studied the application of ILs during minimum quantity lubrication machining of AISI 1045 steel, plain carbon steel and plain medium carbon steel using a CNC vertical machining center with a square-shouldered face milling cutter [10–12]. The ILs used for the study were 1-

methyl 3-butylimidazolium hexafluorophosphate (BMIMPF6), 1-methyl 3-butylimidazolium bis(trifluoromethyl-sulfonyl) imide (BMIMTFSI) and 1-methyl 3-butylimidazolium tetrafluoroborate (BMIMBF4). The results showed that even minute quantity of IL (1% concentration by weight) significantly affects the tribology of the machining process by reducing the surface roughness and resulted in lower average machining forces as compared to dry cutting and conventional flood cooled cutting using minimum quantity lubrication [10–12].

Due to increasing environmental concerns, biodegradable oils need to be used to avoid any environmental hazard caused using petroleum-based lubricants such as mineral oils [15]. Biodegradable oil can be made from plants such as palm, soybean, coconut, sunflower, cottonseed etc. Biodegradable oil can be used as industrial oils, compressor oils, metal working fluids, engine oils, transmission fluids brake oils etc. [15].

Considering all the above-mentioned properties biodegradable oil can also be used as a metal working fluid with an ionic liquid used as an additive to reduce the friction and wear in tribological contacts using minimum quantity lubrication. Khan et al. studied the effect of minimum quantity lubrication on turning AISI 9310 alloy using biodegradable oil based cutting fluid. The results showed 10% reduction in chip-tool interface temperature reducing tool wear and improved surface finish as compared to wet machining [24].

3.5 Problems Faced in Titanium Machining

One potential application of studying the titanium-ceramic contact is that it can be used for reducing the friction and wear in machining of titanium. Titanium machining has its own set of problems which can be listed as described below.

3.5.1 Saw-tooth chips

During the machining of titanium, saw-tooth chips are generally formed. The saw-tooth chips have variable chip thickness. Furthermore, the chip length changes with cutting speed for saw-tooth chips. Lower cutting speeds usually produce shorter chips, whereas higher cutting speeds produce much longer chips. This limits the cutting speed since longer chips are not favored during machining. Longer chips usually get wrapped around the tools that cause downtime and the operator must stop the machine and manually remove the attached chips. This process not only takes time, but the edges of the chips are extremely hot and sharp putting the operators' life at risk. Moreover, the cutting force and cutting temperature increase with the increase of cutting speed. This further restricts the cutting speed for the machining of titanium [16].

3.5.2 High Temperature

Harder materials have higher specific cutting energy which results in producing higher temperatures during machining as compared to softer materials. The higher temperature during machining is generally caused by deformation and friction. The machining temperature is given by the following equation,

$$T = u\sqrt{\frac{vf}{kpc}} \tag{1}$$

where v = cutting speed; f = feed rate; u = specific cutting energy; k = thermal conductivity;

p = density and c = specific heat of the workpiece [16].

From the above equation, increasing the cutting speed or the feed rate will increase the machining temperature. The thermal conductivity of the material should be higher to decrease the machining temperature, but the thermal conductivity of titanium alloy is about 18.67 W/m°C at 1000°C which is very low as compared to the thermal conductivity of steel which is about 381.77 W/m°C [16]. Due to the above-mentioned factors, almost 80% of the heat generated is conducted into the tool during machining of Ti-6Al-4V. Furthermore, due to the higher temperatures different types of cutting tool degradation processes, especially chemical reaction is promoted in this favorable environment. These high cutting temperatures and chemical reaction reduce the tool life, surface quality of workpiece and cutting accuracy of the tool due to tool degradation.

3.5.3 High Stress on cutting tools

Reduction in contact surfaces and low plasticity of titanium alloys causes high stresses on the cutting edge. Figure 1. shows the typical stress distribution on cutting tool chip when the saw-tooth chips are formed.

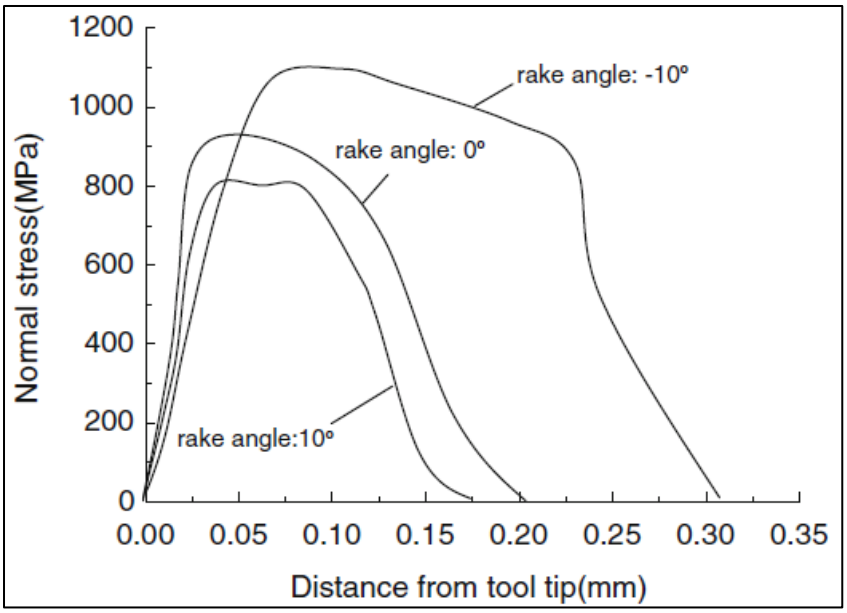

Figure 4: Normal stresses for saw-tooth chips at chip-tool surface for different rake angles [16].

From figure 1, the highest stress occurs at the closest distance from the tooltip. The distance having zero nominal stress goes on increasing with the decreasing rake angle of the tool. Moreover, the strength and hardness of titanium do not reduce at higher temperatures which results in higher stress at higher temperatures on cutting tools leading them to wear out rapidly.

3.5.4 High tool wear

As mentioned in the earlier sections, the high and pulsating pressure and stress, high temperature and friction cause the degradation of the tool leading to tool wear. Almost all types of cutting tools like the straight tungsten carbide tool, cemented Titanium Nitride (TiN) tool, pure aluminum oxide type of ceramic tool, Titanium Carbide (TiC) coated tool, alloyed cemented carbide tool, alloyed chemical vapor deposition (CVD) - coated carbide tool, binderless cubic boron nitride (CBN), sintered diamond tool and natural diamond tool have been tested in the laboratories. However, only carbide, sintered diamond, natural diamond and binderless CBN

tools have shown acceptable performance [16]. The main causes of tool wear for different cutting tools are coating delamination, adhesion, attrition, diffusion, plastic deformation and cracks.

3.5.5 Application of cutting fluid as coolant

Cutting fluid is a type of lubricant used for machining. Cutting fluids can be applied in four ways namely flood lubrication, cryogenic cooling, MQL and MQCL.

a. *Flood lubrication:* It is the conventional method of applying cutting fluids. It uses a flow rate of over 100 L/h. Due to high heat transfer capabilities and being economical, water-based emulsions are generally used for flood lubrication. The cooling is mainly due to convection of heat from the machining zone, and only a small quantity of the lubricant may reach the tool-chip interface. High pressure coolant delivery systems are preferred as the low-pressure coolant is not able to break through the vapor blanket formed by prevalent high temperatures. Moreover, the high pressure helps in chip breaking thus reducing friction by preventing excessive contact between the chip and the tool [2]. However, the use of high-pressure lubricant delivery system causes increased consumption of the lubricant that causes serious environmental damage due to the presence of the non-biodegradable ingredients in cutting fluids like the EP additives and the emulsifiers.

b. *Cryogenic cooling:* Cryogenic cooling makes the use of coolant or lubricant below -150°C. Nitrogen is popularly used since it is non-toxic and available in abundance. It is much better than any other technique in terms of reducing the cutting temperature [2] and thus increasing the cutting speed. But, the extreme cooling causes hardening of the workpiece causing higher cutting forces and ultimately resulting in poor surface finish and dimensional inaccuracy.

c. *Minimum Quantity Lubrication (MQL):* It involves the application of low quantity of the cutting fluid, eliminating the disposal of lubricant issue face in flood lubrication as almost all the fluid is evaporated. It can be applied in two forms i.e. drop-by-drop or mist form [25–27]. The application of MQL in mist form is the one being popular [2]. It involves the atomization of the fluid by mixing it with compressed air and applied as an aerosol spray which increases the surface area of the applied lubricant which in return helps in better cooling. Moreover, the lubricant reaches the tool-chip interface through capillarity and forms a thin film at the interface.

d. *Minimum Quantity Cooled Lubrication (MQCL):* This technique is the combination of MQL and cryogenic cooling. Using MQL a cooled lubricant is applied on the workpiece to be machined. It has shown to be effective in reducing the temperature and assisting in chip breaking [2], but however cryogenic cooling leads to increased cutting forces resulting in poor surface finish.

e. *Atomization based cutting fluid:* This method uses a metal-working fluid (MWF) that is water soluble mixed with high velocity gas called air-CO_2 mixture at 1-2°C applied using an ACF spray unit that consists of an ultrasonic vibration-based atomizer, MWF reservoir with a delivery tube, a nozzle unit and high-pressure gas delivery [28]. Shiv G. Kapoor et al., found that the ideal concentration for ACF is 10% [28]. ACF reduces the mean cutting temperature by 7-13% as compared to 1-3% provided by flood lubrication [29]. The temperature measurement at the tool-chip interface shows that ACF penetrates the tool-chip interface more efficiently improving the tool life [29].

4.0 OBJECTIVES OF THE PROPOSED WORK

1. To study the tribological properties of titanium-ceramic contact experimentally to reduce the friction and wear.
2. To study the performance of protic ionic liquid used as an additive to biodegradable oil in starved lubrication regime.

5.0 PRELIMINARY WORK

5.1 Heater Set Up for the Current Reciprocating Tribometer

The ball-on-flat reciprocating tribometer designed and built by a group of students under the guidance of Dr. Patricia Iglesias had capability to work only at room temperature due to the lack of a heater to heat the samples under test. In any mechanical contact, friction generates heat; increasing the temperature at the point of contact. The physical properties like viscosity of any lubricant are altered at higher temperatures. Lubricant is used to reduce the friction at the point of contact and is thus subjected to higher temperatures. Hence, it is very necessary to know the response of the lubricant at higher temperature. It is essential to validate the effect of the ionic liquid used as an additive in the lubricant at higher temperature. A heater system was designed and manufactured to validate the effect of ionic liquid up to 700° C. The design of the heater system included the band heater, a Proportional Integral Derivative (PID) Controller as the power source, a K-Type thermocouple to measure the temperature at the surface of the sample under test and the sample and heater holder. The Sample and heater holder were manufactured in the machine shop.

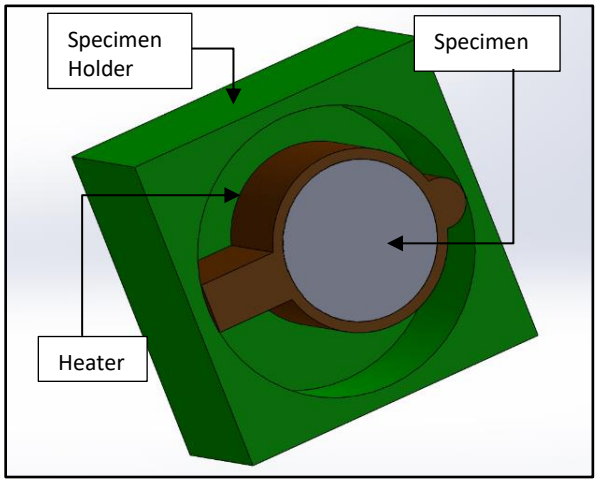

Figure 5: CAD model of heater set up in the specimen holder.

5.1.1 Mineral Wool Insulation

The air gap formed due to the bump formed by the terminals on both the sides of the heater would have adversely affected the heater performance. Mineral wool insulation was a perfect choice for insulating the entire system for minimizing the heat losses in the system. The operating temperature range for the wool insulation was up to 650°C (1200°F). The wool insulation was also tested in the machine shop by heating it with a flame torch which heated the wool insulation up to almost 600°C (1100°F) and the insulation sustained that temperature with ease.

Figure 6: Mineral Wool Insulation.

5.1.2 High temperature Bonding Cement

The thermocouple is glued to the sample under test using a high temperature cement called "OMEGABOND 400". This cement is not affected by the high temperatures of the tests and it does not react with the lubricant in use. The cement was selected based on its easy availability, ease of use and cheap value.

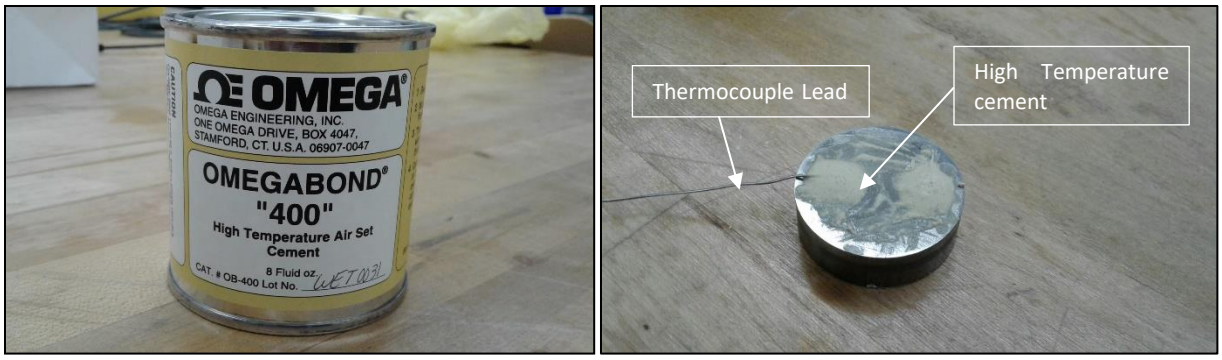

Figure 7: High temperature cement used as glue for the thermocouple.

5.2 Performing tests using the heater system

After testing the entire heating set up and making the necessary changes like reducing the weight of the specimen holder and adding screws to provide support for clamping, tests were carried out on the reciprocating ball-on-flat tribometer at 100° C using mineral oil, neat ionic liquid and 1% ionic liquid with mineral oil as lubricant to verify the effect of temperature on the performance of ionic liquid. The tribocontact used for the test was between 1018 steel disks and AISI 420C balls. The Ionic liquid under test was Trihexyl(tetradecyl)phosphonium bis(2,4,4-trimetylpentyl) phosphinate- [THTDP][Phos]. Previous results of Dr. Patricia Iglesias' group show impressive friction and wear reduction using [THTDP][Phos] as a neat lubricant [30]. Therefore, the tests were performed at 100°C with 1080 and the results from previous work were used as data for tests at 25°C [30].

The parameters used for the test were as follows:

Stroke=5mm; Load=2N; Frequency=5 Hz; Sliding Distance= 200 m.

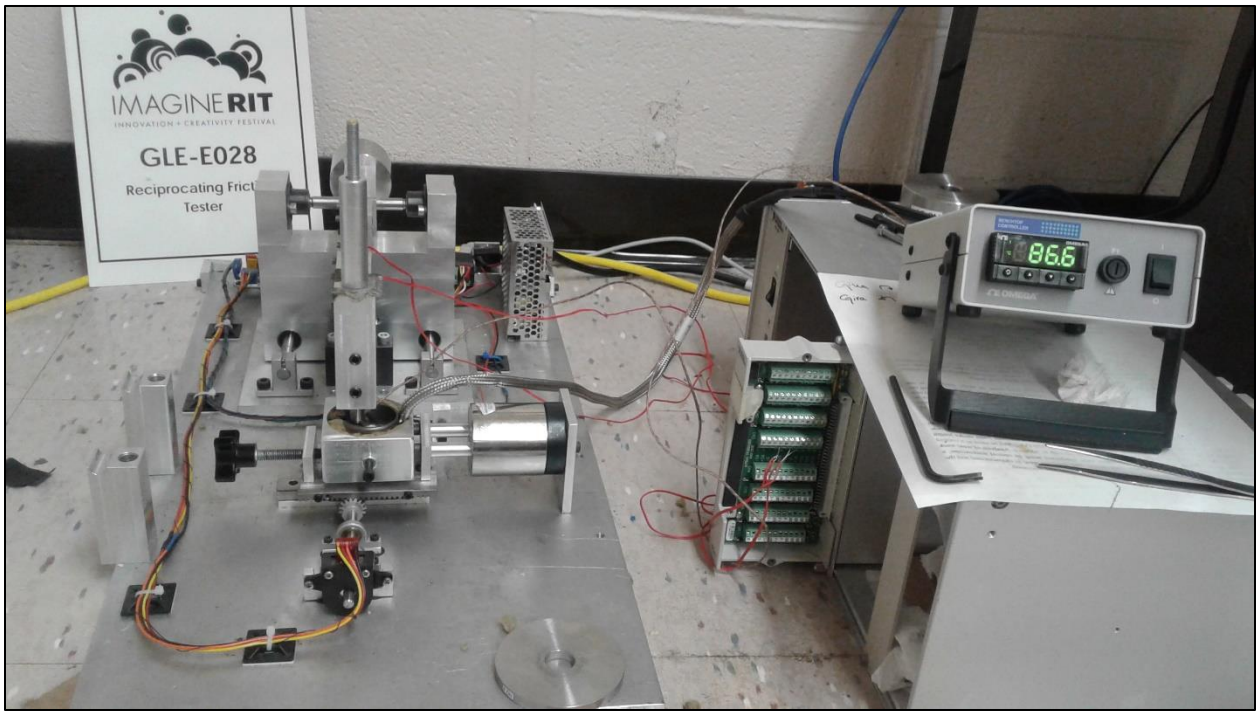

Figure 8: Performing test with the heater set up assembled.

5.2.1 Results

5.2.1.1 Friction Coefficient Analysis

Figure 9 shows the comparison of friction coefficient using MO, [THTDP][Phos] and 1% [THTDP][Phos] in MO. At 25°C the IL used as neat lubricant as well as an additive to MO reduced the friction coefficient as compared to MO as neat lubricant. But, on the contrary at 100°C it was not very effective in reducing the friction coefficient both as a neat lubricant or as an additive. These results clearly show the effect of temperature on the performance of IL in reducing friction.

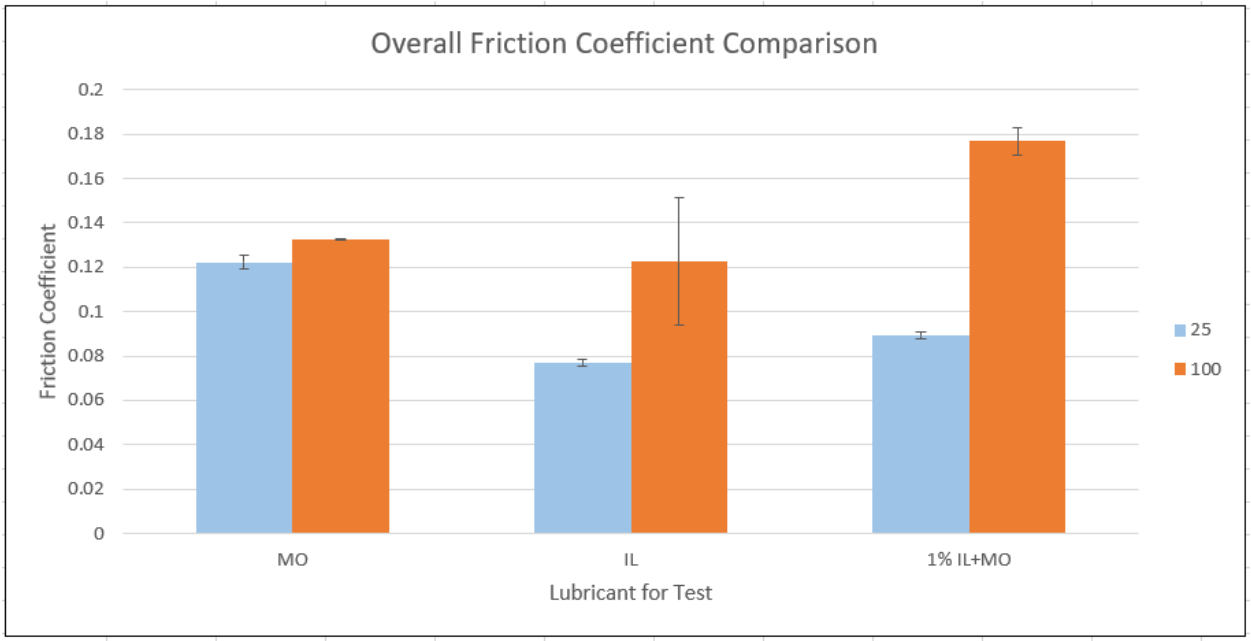

Figure 9: Comparison of Friction Coefficients at 25°C and 100°C.

Table 3. compares the friction coefficient of different tests conducted to compare the tribological performance of these three lubricants.

Table 1: Overall summary of friction coefficient at 25°C and 100°C.

Temperature	Mineral Oil	Neat IL	1% IL+MO
25°C	0.1224	0.0768	0.0892
100°C	0.1327	0.1225	0.1767

Figure 10 gives the plot of friction coefficient with respect to time for both the tests with MO as lubricant. The sudden spikes in the graph can be because of some debris on the disk.

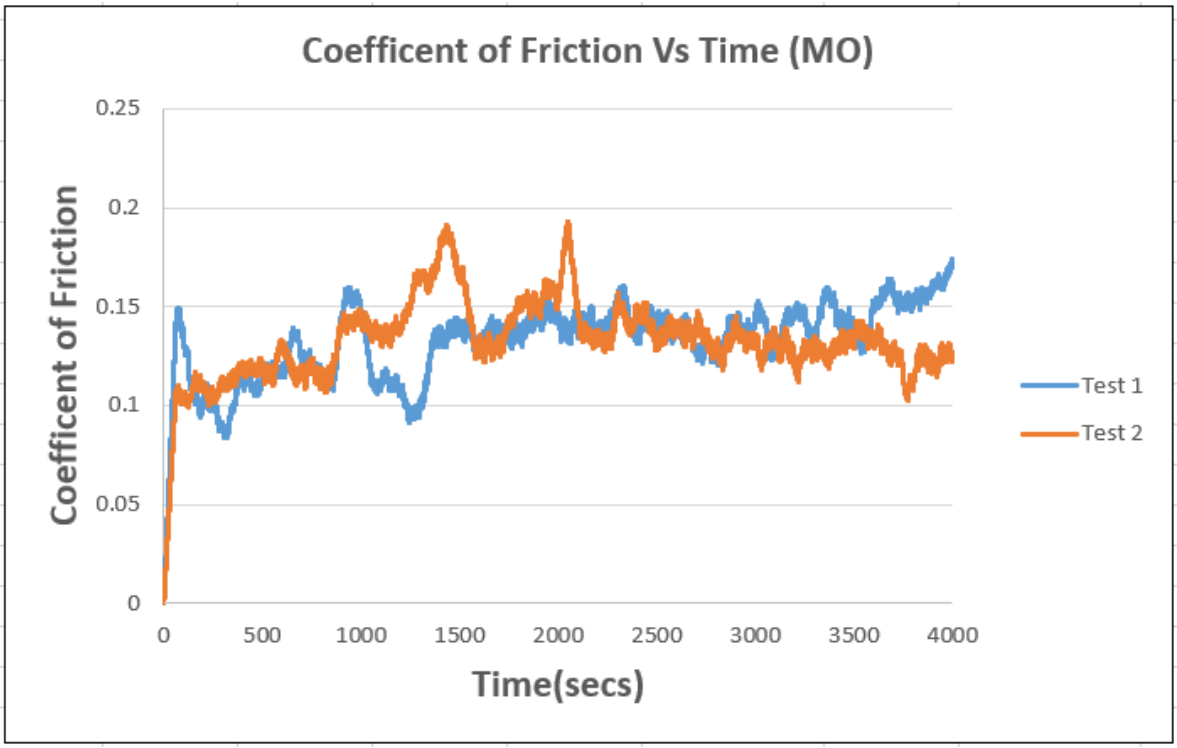

Figure 10: Friction Coefficient Vs Time (MO).

Figure 11 shown below gives the plot of friction coefficient with respect to time for all the three tests with IL as lubricant.

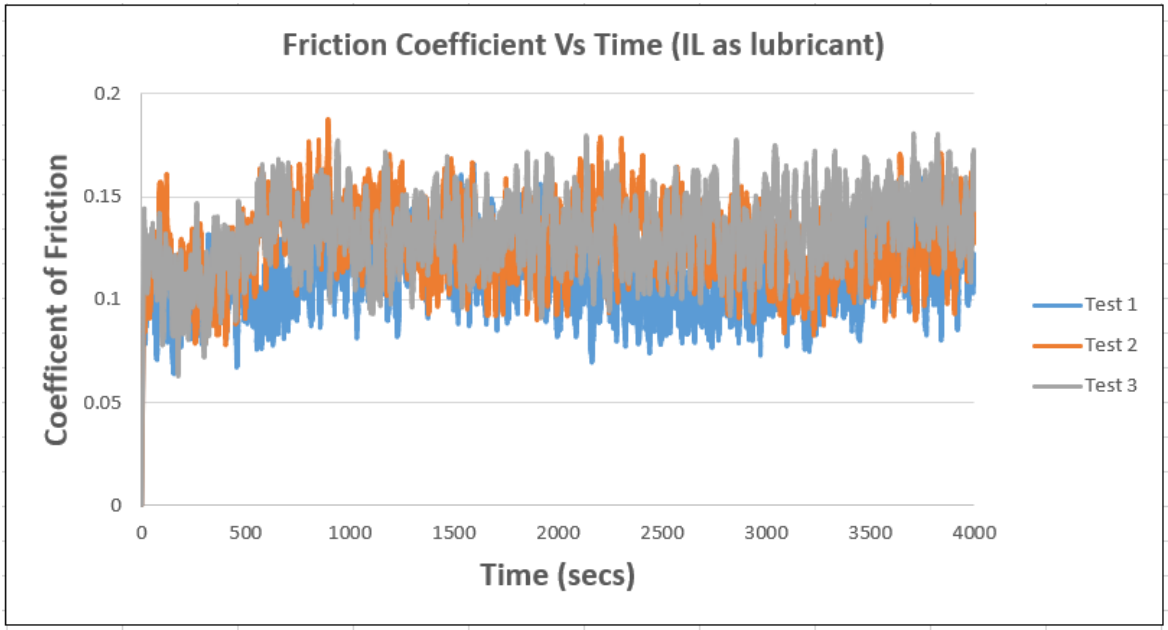

Figure 11: Friction Coefficient Vs Time (Neat IL).

Figure 12. gives the plot of friction coefficient with respect to time for both the tests conducted with 1% IL with MO as lubricant. The sudden spikes in the graph can be because of some debris on the disk.

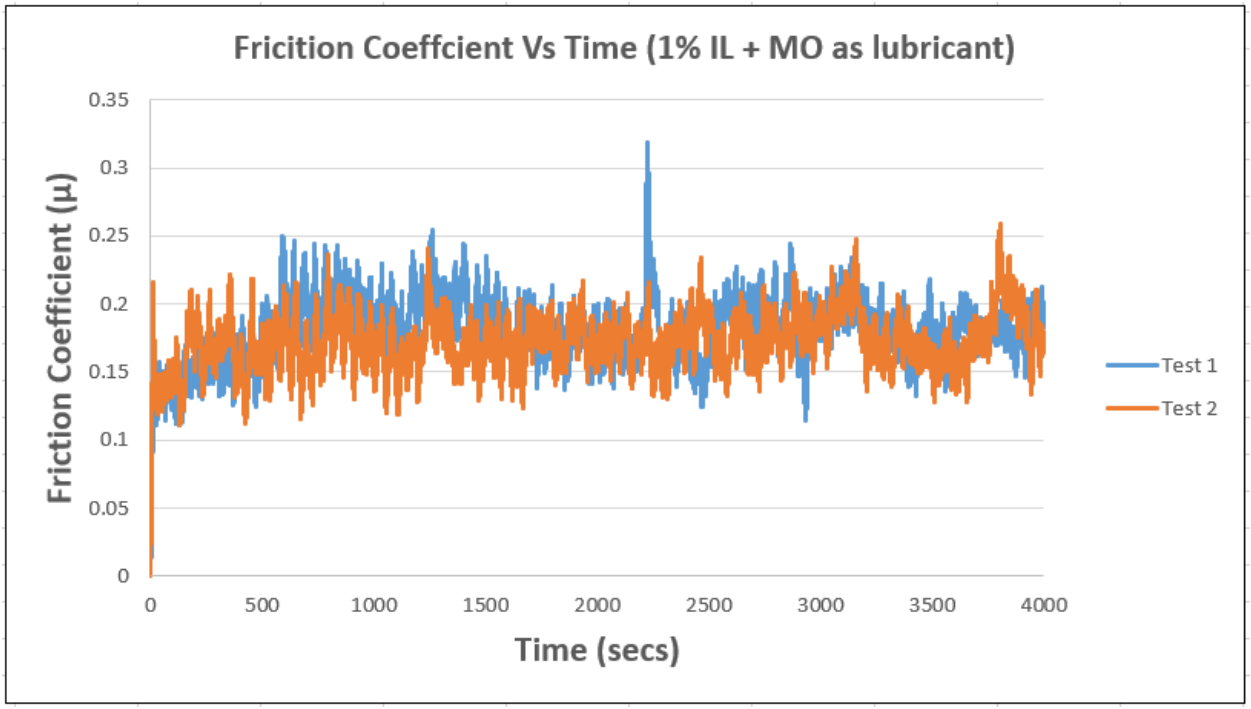

Figure 12: Friction Coefficient Vs Time (1% IL+MO).

5.2.1.2 Wear Volume Calculations

Wear Volume was calculated using the formulae given by J. Qu and J. Truhan [31] using MATLAB.

$$V_f = L_s \left[R_f^2 \arcsin\left(\frac{W}{2R_f}\right) - \frac{W}{2}(R_f - h_f)\right] + \frac{\pi}{3} h_f^2 (3R_f - h_f) \quad (2)$$

$$h_f = R_f - \sqrt{R_f^2 - \frac{W^2}{4}}; \quad (3)$$

Where V_f = Wear Volume in mm^3;

h_f = depth of the wear track;

L_s = Stroke length in mm;

W = track width in mm;

R_f = radius of the ball used;

The track width was measured using “OLYMPUS B-2” optical microscope.

Table 2: Wear Volume in mm^3 using different lubricants for the tests.

Temperature	Mineral Oil	Neat Ionic Liquid	1% IL+MO
25°C	0.0151	0.0080	0.0123
100°C	0.0096	0.0172	0.0183

5.2.2 Conclusion

Tests were conducted at 25°C [30] and 100°C using MO, Neat IL and 1% IL in MO as lubricants in the tribocontact of 1018 steel disks and AISI 420C steel balls. The use of mineral oil at 25°C and 100°C did not show significant change in friction coefficient. But, the use of IL as neat lubricant as well as an additive demonstrated the effect of change in viscosity on friction coefficient due to change in temperature of the lubricant. The friction coefficient increased with the increased temperature of the lubricant. This showed that [THTDP][Phos] does not have good effect in terms of reducing friction at higher temperature.

5.3 Preliminary Tests on Ti6Al4V

Tests were conducted on Ti6Al4V disks using ball-on-flat reciprocating tribometer. Two types of lubricants were used to perform the tests which were Mineral oil and Tri-[bis(2-hydroxyethylammonium)] Citrate (DCi) used as an additive with base oil.

The test parameters used for the tests were as follows:

Stroke = 6 mm; Load = 2N; Frequency = 5 Hz; Sliding Distance = 432 m;

Mean contact pressure = 1.10 GPa; Max Contact pressure = 1.65 GPa

5.3.1 Results

The results showed a friction reduction of 5% using 1% wt. DCi as compared to mineral oil as lubricant. Only one type of IL was used for the preliminary tests. Different type of IL with different concentrations can yield better results than DCi. Figure 13 shows the comparison of friction coefficient using MO and 1% DCi. The average friction coefficient using 1% DCi with MO was 0.1643 as compared to 0.1731 achieved using MO as neat lubricant.

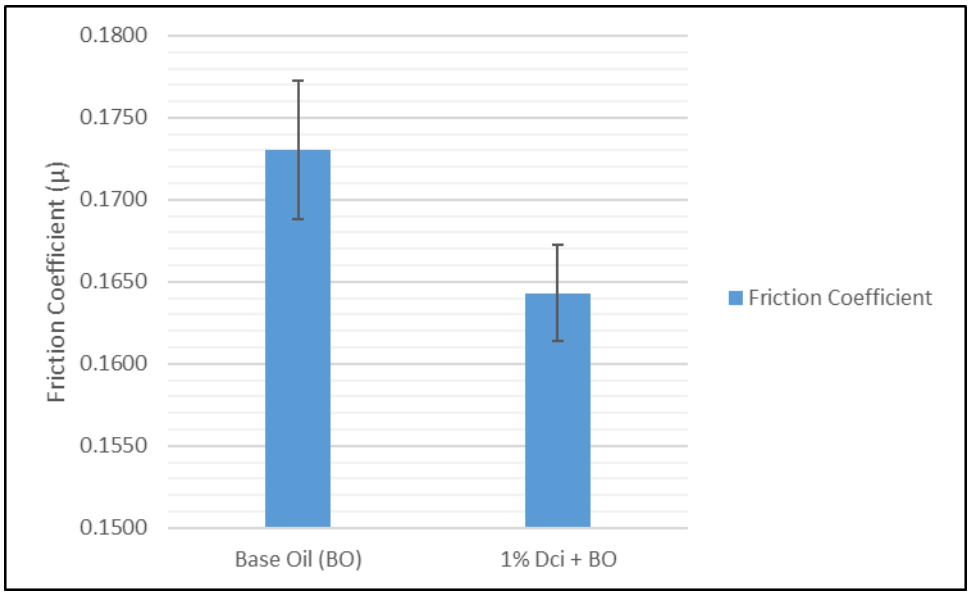

Figure 13: Comparison of Friction Coefficient Using MO and 1% DCi + MO.

Table 5. compares the friction coefficient of different tests conducted to compare the tribological performance of these two lubricants.

Table 3: Comparison of friction coefficient.

Test No.	Mineral Oil	1% DCi + MO
1	0.1701	0.1622
2	0.1760	0.1664

Figure 14. shows the friction coefficient response with respect to time for both the tests using MO as neat lubricant.

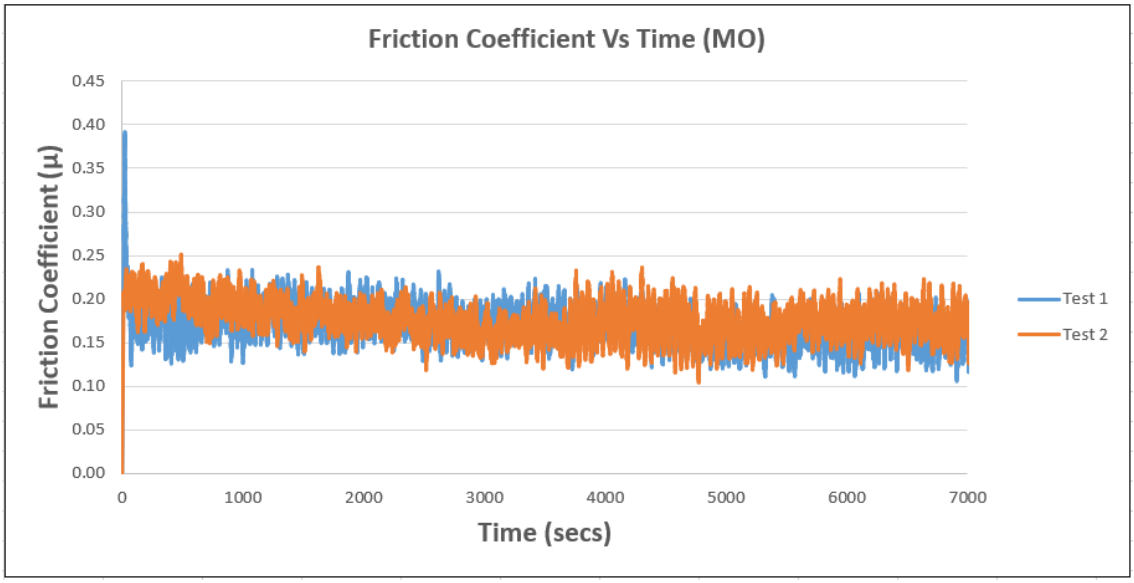

Figure 14: Friction Coefficient Vs Time (MO).

Figure 15. shows the friction coefficient response with respect to time for both the tests using 1% DCi with MO as lubricant.

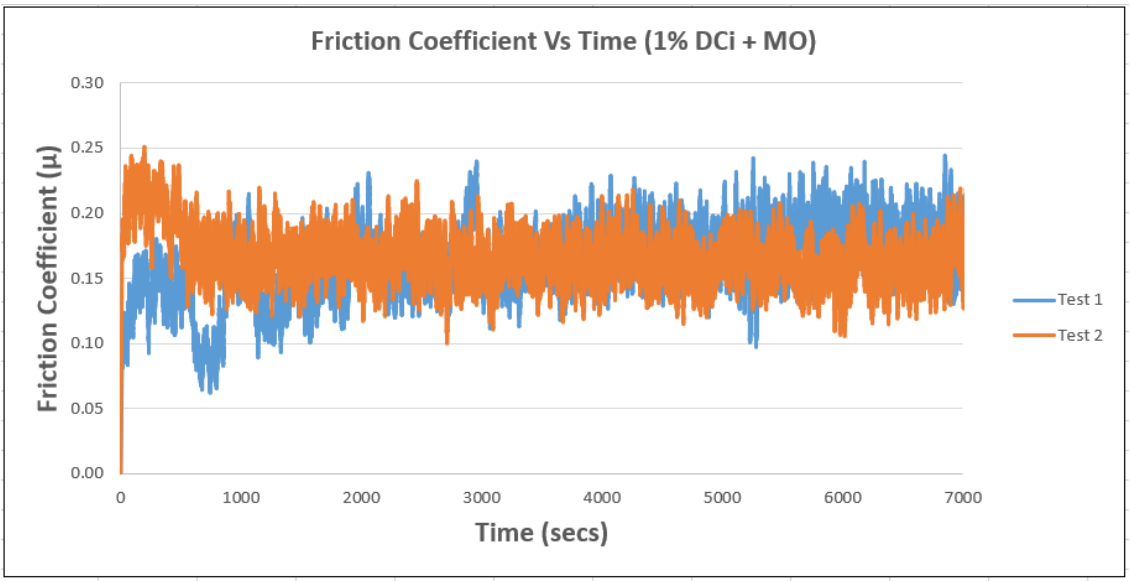

Figure 15: Friction Coefficient Vs Time (1% DCi + MO).

6.0 EXPERIMENTAL WORK

6.1 Materials and Methods

6.1.1 Sample Disk and Ball Material Properties

Ti6Al4V is the most commonly used titanium alloy. Therefore, Ti6Al4V titanium sample disks, 1.25 inches in diameter was used as the sample disks for the tests. These disks were in contact with a Tungsten Carbide ball which is 1.5 mm/ 0.0591 inches in diameter. The material properties of both the titanium disks and Tungsten Carbide balls can be seen in Table 6 below.

Table 4: Material Properties of Sample Disk and Ball.

		Material Properties			**Material Dimensions**	
	Grade	**Elastic Modulus (GPa)**	**Poisson's Ratio**	**Hardness**	**Diameter (mm)**	**Thickness (mm)**
Disk	Grade 5	113.8	0.342	36 HRC	31.75	25.4
Ball	G25	686	0.2 - 0.22	90 HRB	1.5	N/A

The material dimensions were selected based on the experimental set-up. The pin used to hold the ball can only accommodate a 1.5 mm ball and the fixture used to hold the disk in place can only accommodate 1.25 inches/ 31.75 mm disk. The tungsten carbide ball diameter can be changed if higher contact pressures are required.

6.1.2 Lubricant Properties

Two types of fluids were used in combination as lubricant for conducting the experiments. They were as follows:

1. Biodegradable oil used as base lubricant: Biotelex 46
2. IL used as an additive: Tri-[bis(2-hydroxyethylammonium)] Citrate (DCi)

Bio Telex 46 was the base fluid used as the lubricant for this study. It was provided by REPSOL YPF Lubricantes y Especialidades, S.A. Bio Telex 46 is a biodegradable oil which has passed all the required biodegradability and ecotoxicity tests as required by the Eco-Label Certification. This was the main reason to select this particular type of oil as the lubricant as it was bio-degradable. The technical specification of Bio Telex 46 is given in Table 7 below.

Table 5: Technical Specifications of Bio Telex 46 [32].

Properties	**Method**	**Unit**	**Value**
Density at 15°C	ASTM D 4052	g/cm^3	0.912
Viscosity at 100°C	ASTM D 445	mm^2/s	9.8
Viscosity at 40°C	ASTM D 445	mm^2/s	46
Viscosity Index	ASTM D 2270	-	180
Pour Point	ASTM D 97	°C	-45
Flash Point, V/A	ASTM D 92	-	310
Foams (stability)	ASTM D 892	mL	0/ 0/ 0
Low temperature fluidity. -20°C, 168h	ASTM D 2532	%	1.868

Tri-[bis(2-hydroxyethylammonium)] Citrate (DCi) was synthesized at RIT by the team in the tribology lab and was used as the IL in concentration of 1% by wt. as an additive to the biodegradable oil for the tungsten carbide tests.

The summary of the procedure used for the synthesis of DCi is as follows:

1. 0.6 mole of Diethanol Amine was dissolved in 100ml of ethanol to form a liquid mixture and the mixture was poured into a 500ml round bottom flask. A magnetic stirrer was placed under the round bottom flask to homogenize the mixture.

2. After that 0.2ml Citric acid was dissolved in 100ml of ethanol.

3. A pressure equalizing additional funnel was connected to the round bottom flask to add the Citric acid and ethanol mixture. The mixture was transferred to the pressure equalizing additional funnel and added dropwise to the round bottom flask in around 100min. Compressed Argon gas was selected as the protective gas during the reaction process.

4. A reflux condenser was connected to the round bottom flask to mitigate the heat generated during the chemical reaction.

5. After the reaction, the solvent of ethanol that suspended in the upper layer was pulled to a beaker and the product was removed to a flask.

6. The flask was then placed in a water bath at 78℃ to eliminate the remaining ethanol inside the product.

7. Finally, to get rid of the ethanol completely, the product was evaporated again by vacuum line for 7 hours.

6.1.3 Sample Preparation

The disk samples are prepared from a rod of Ti6Al4V. Firstly, 1-inch/ 25.4 mm long disks are cut using a cutting wheel. Now, one of the faces of this disk is polished to make the disk ready for use in the experiment. Polishing the disk is a 6-step process which includes the use of 6 different polishing papers with different roughness. The different roughness values for the 6 polishing disks are as follows:

1. MD- 220 (220 µ grain size)
2. MD – 500 (500 µ grain size)
3. MD – 1200 (1200 µ grain size)
4. 9 µ
5. 3 µ
6. 1 µ

The surface roughness of the polished face of the disk is measured using a non-contact type "Veeco Profilometer".

6.2 Experimental Set-up

The ball-on-flat reciprocating tribometer was used for performing the tests. This reciprocating tribometer was used to characterize the friction and wear properties of Ti6Al4V. The test set-up can be seen in Figure 16 below.

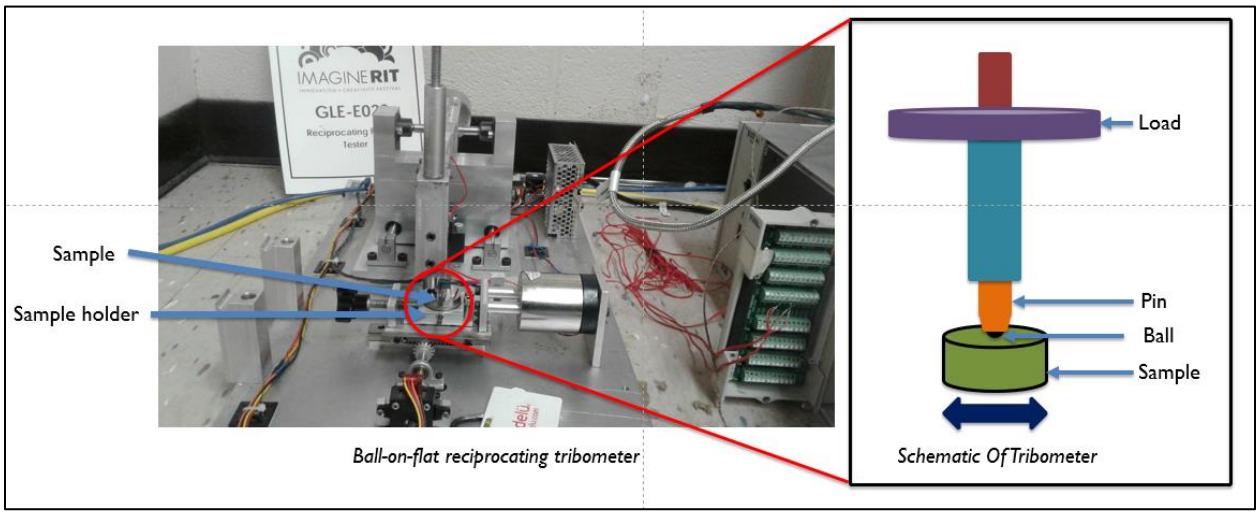

Figure 16: Ball-on-Flat Reciprocating Tribometer.

As can be seen in Figure 16, the ball-on-flat reciprocating tribometer consists of a pin which is holding a protruding ball. This ball is in contact with the sample disk whose friction and wear characteristics are under study. A load is applied on top of the pin as shown in Figure 16. The sample disk reciprocates back and forth to generate friction in between the ball and the disk. The stroke and frequency of the reciprocating action and the time of test can be varied to control the sliding distance and sliding speed. The lubricant is applied by using a pipette on the surface of the disk between the ball and the sample disk. Only 1-2 mL of lubricant is used to simulate minimum quantity lubricant (MQL) type of lubrication. Loads of 1N, 2N and 3N resulting in a contact pressure of 0.88 GPa, 1.1 GPa and 1.26 GPa were applied on the pin for the tests.

The contact pressure is calculated by the equation given below;

$$P_{max} = \frac{3F}{2\pi a^2}\ ; \qquad a = \sqrt[3]{\frac{3F\left[\frac{1-\nu_1^2}{E1} + \frac{1-\nu_2^2}{E2}\right]}{4\left(\frac{1}{R1}+\frac{1}{R2}\right)}} \tag{4}$$

Where F = applied load

ν_1 = Poisson's ratio of ball

ν_2 = Poisson's ratio of disk

E_1 = elastic modulus of ball

E_2 = elastic modulus of disk

R_1 = radius of ball

R_2 = radius of disk

All these required parameters to calculate the contact pressure for the tests can be found in Table 6.

6.3 Experimental Parameters

The ball-on-flat reciprocating tribometer has two dependent parameters i.e. sliding distance and sliding speed which are dependent on 3 variables which are as follows:

a) Stroke

b) Frequency

c) Testing Time

Contact pressure is the third parameter which is dependent only on the applied load and is independent from the 3 variables mentioned above.

In this study, only frequency and load were varied, and the remaining variables were kept constant. Frequencies of 3 Hz, 4 Hz and 5 Hz were used at different loads. A Load of 2N was used for frequency of 3 Hz, 4 Hz and 5 Hz. Additionally, the frequency of 5 Hz was also tested at load of 1N and 3N. The stroke was kept constant at 6 mm. The sliding distance was kept constant at 432 m by adjusting the test time from 120 mins to 200 mins. The test matrix used for this study can be seen in Table 8 and Table 9.

Table 6: Experimental Parameters Used: Frequency Based Testing.

Stroke (mm)	Frequency (Hz)	Sliding Distance (m)	Test Run Time (Mins)	Sliding Speed (m/s)	Load (N)	Contact Pressure (GPa)
6	3	432	200	0.036	2	1.1
6	4	432	150	0.048	2	1.1
6	5	432	120	0.06	2	1.1

Table 7: Experimental Test Parameters: Load Based Testing.

Stroke (mm)	Frequency (Hz)	Sliding Distance (m)	Test Run Time (Mins)	Sliding Speed (m/s)	Load (N)	Contact Pressure (GPa)
6	5	432	120	0.06	1	0.88
6	5	432	120	0.06	2	1.1
6	5	432	120	0.06	3	1.26

The testing matrix was developed in an effort towards finding the parameters resulting in the highest reduction of friction coefficient and wear Volume. Therefore, load-based testing was conducted based on the results of frequency-based testing.

6.4 Friction Calculation

The friction coefficient is calculated with help of a LabVIEW program using two KYOWA KFGS-2-120-C1-11L3M2R strain gauges connected in a half bridge configuration. The strain gauges are connected to the arm of the reciprocating tribometer as shown in Figure 17 and measure the resistance force offered to the reciprocating motion. The strain gauges are connected to the SCXI-1000 Universal Strain Gauge Module.

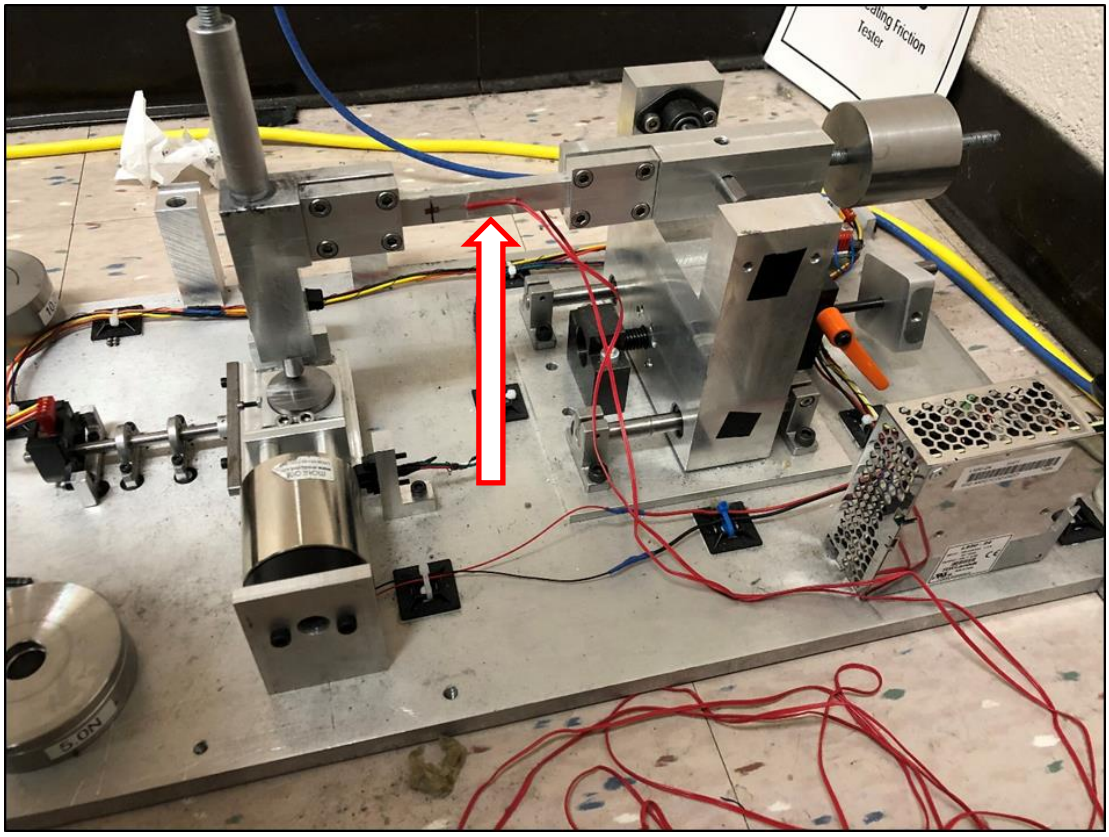

Figure 17: Strain gauges connected to the arm.

The friction coefficient is calculated by the LabVIEW program using the formula given below,

$$F = \frac{w * h^2 * E * Strain}{6 * L} \quad (5)$$

Where F = Resistance force

w = Width of the arm

h = Height of the arm

E = Elastic Modulus

L = Length of the arm

6.4 Wear Volume Calculation

Wear Volume was calculated using the formulae given by J. Qu and J. Truhan [31] using MATLAB.

$$V_f = L_s \left[R_f^2 \arcsin\left(\frac{W}{2R_f}\right) - \frac{W}{2}(R_f - h_f)\right] + \frac{\pi}{3} h_f^2 (3R_f - h_f) \quad (2)$$

$$h_f = R_f - \sqrt{R_f^2 - \frac{W^2}{4}}; \quad (3)$$

Where V_f = Wear Volume in mm^3; W = track width in mm;

h_f = depth of the wear track; R_f = radius of the ball used;

L_s = Stroke length in mm;

The track width was measured using “OLYMPUS B-2” optical microscope.

7.0 RESULTS AND DISCUSSION

Experiments were performed using Bio telex 46/ biodegradable oil (BO) and 1% Tri-[bis(2-hydroxyethylammonium)] Citrate (DCi) in BO as lubricant on the ball-on-flat reciprocating tribometer. The ball is constrained using a pin and thus has a slip ratio of 1. Slip ratio can be defined as the ratio of the difference between sliding velocity of the disk and the angular velocity of the ball and the sliding velocity which can be mathematically given as follows:

$$\text{Slip ratio} = \frac{u - r\omega}{u} \quad (6)$$

Where u = Sliding speed of the disk

r = radius of the ball

ω = angular velocity of the ball [33]

The coefficient of friction and wear volume were calculated and compared for these two lubricants. As can be seen from Table 8, the testing was performed using two variables which were frequency and load.

7.1 Frequency Based Testing:

7.1.1 Friction Coefficient

The first variable in the test matrix was the frequency of the reciprocating action of the ball-on-flat reciprocating tribometer. Testing was performed at 3Hz, 4Hz and 5 Hz respectively. All the other parameters used for this testing can be seen in Table 8. The initial testing was performed with a load of 2N and at a frequency of 3Hz, 4Hz and 5Hz. The maximum friction reduction of almost 50% was seen at frequency of 5Hz. Therefore, additional testing was conducted at this

frequency at loads of 1N and 3N to observe the change in friction reduction with the change in the contact pressure. Furthermore, it was also seen that the sudden spike in friction coefficient while using 1% wt. DCi comes much later in time as compared to using BO as lubricant. Results showed a maximum friction reduction of 50% using 1% wt. DCi in BO as compared to BO as the lubricant. Figure 18 shows the comparison of friction coefficient using BO and 1% wt. DCi as an additive to BO.

As can be seen in Figure 18 the friction coefficient at frequency of 3 Hz and 4 Hz with BO as the lubricant is almost the same the friction coefficient with 1% DCi with BO as the lubricant. No significant friction reduction was seen at frequency of 3 Hz and 4 Hz.

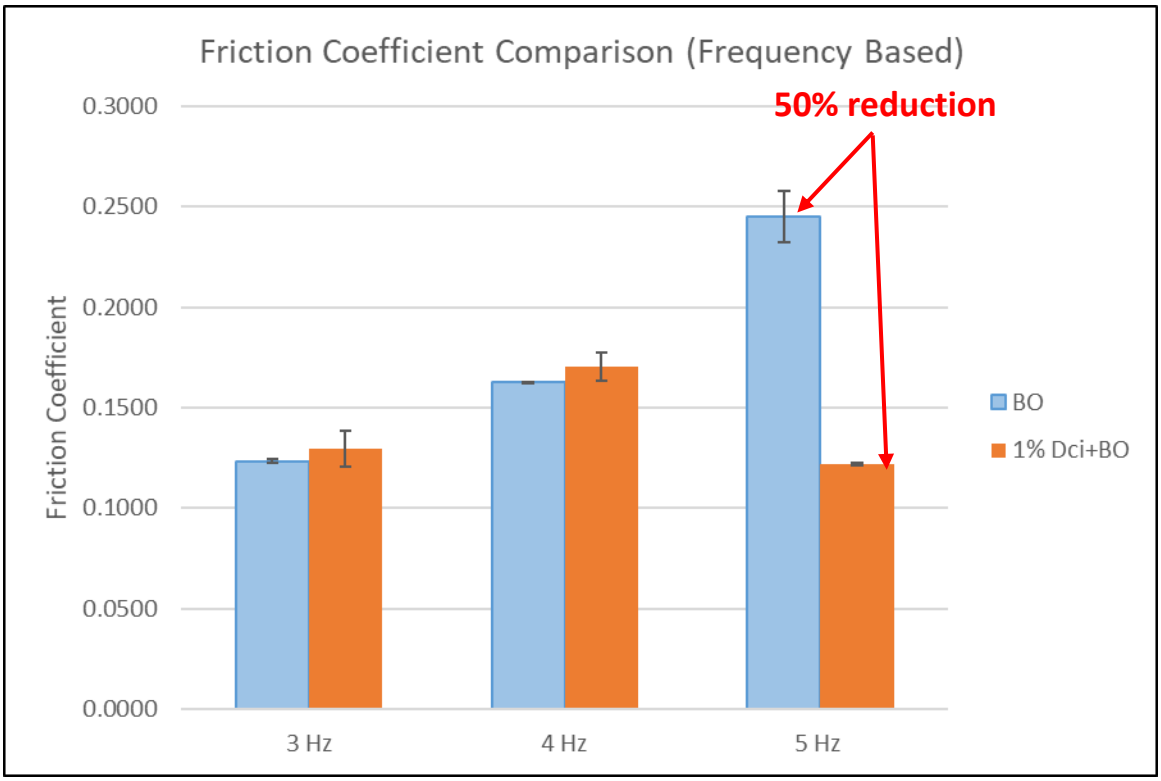

Figure 18: Comparison of Friction Coefficient Using BO and 1% DCi + BO.

Table 10. compares the friction coefficient of different tests conducted to compare the tribological performance of these two lubricants.

Table 8: Comparison of Friction Coefficient: Frequency Based.

Lubricant	Frequency		
	3 Hz	4 Hz	5 Hz
BO	0.1234 (0.001216)	0.1626 (6.38E-05)	0.2452 (0.012673)
1% wt. DCi + BO	0.1295 (0.008762)	0.1704 (0.006986)	0.1219 (0.000722)

The friction coefficient response with response to time was plotted for all the tests conducted with both lubricants at 3 different frequencies.

Figure 19 shows the friction coefficient response with respect to time for both the tests conducted using BO as neat lubricant at 3 Hz.

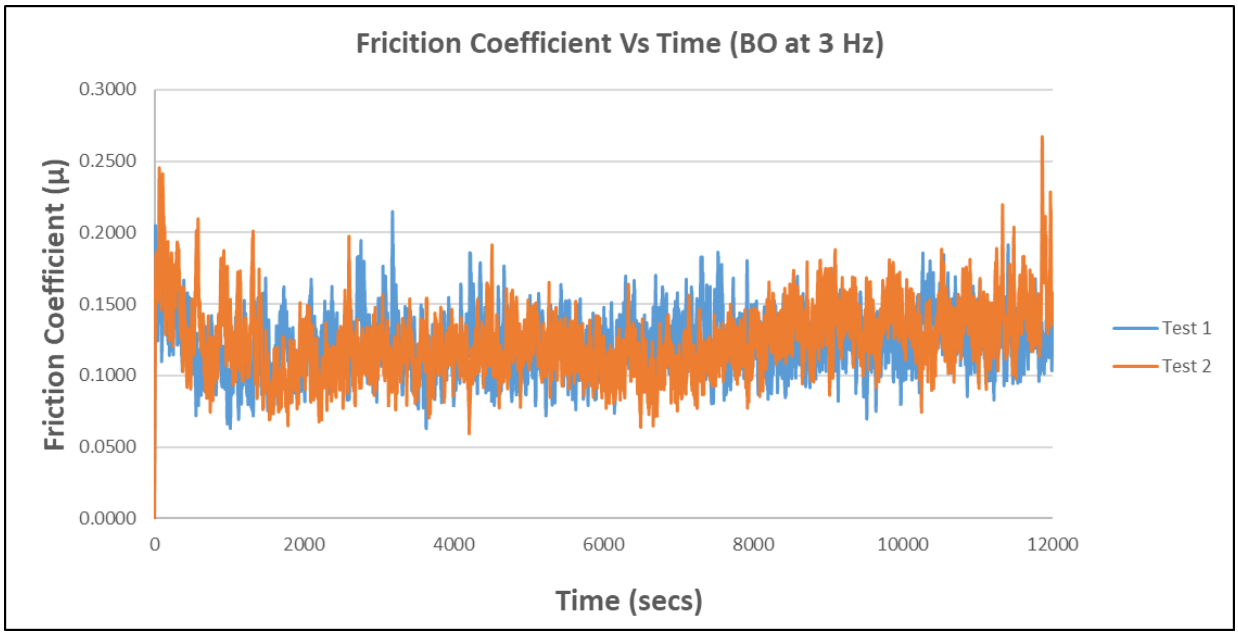

Figure 19: Friction Coefficient Vs Time (BO at 3 Hz).

Figure 20 shows the friction coefficient response with respect to time for all the 3 tests conducted using 1% wt. DCi with BO as lubricant as 3 Hz.

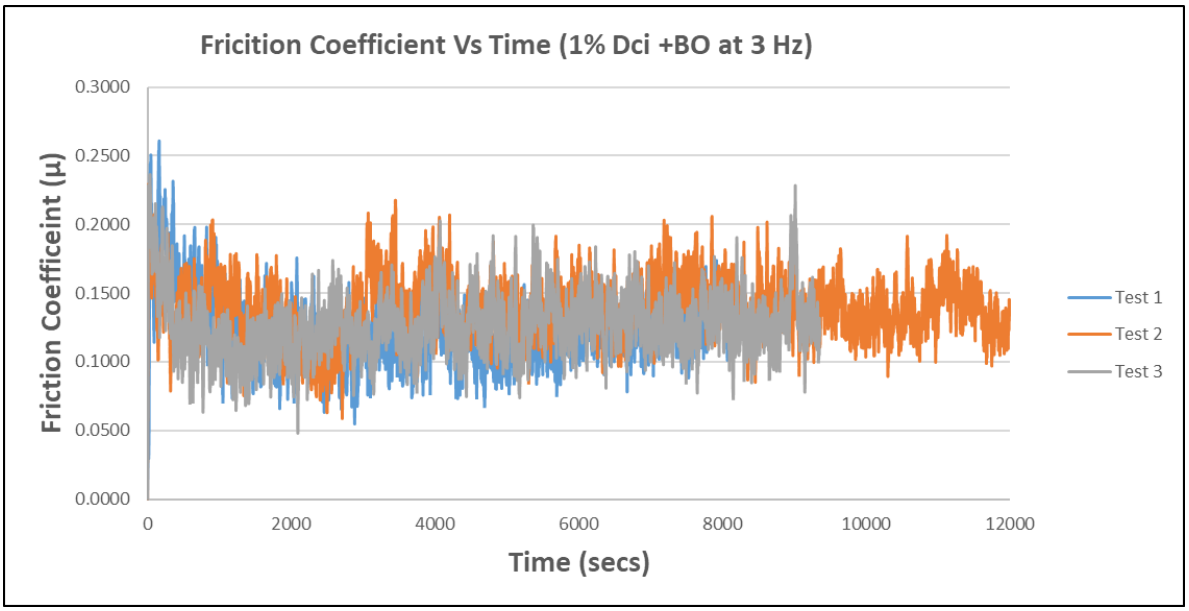

Figure 20: Friction Coefficient Vs Time (1% DCi + BO at 3 Hz).

Figure 21. shows the friction coefficient response with respect to time for both the tests conducted using BO as neat lubricant at 4 Hz.

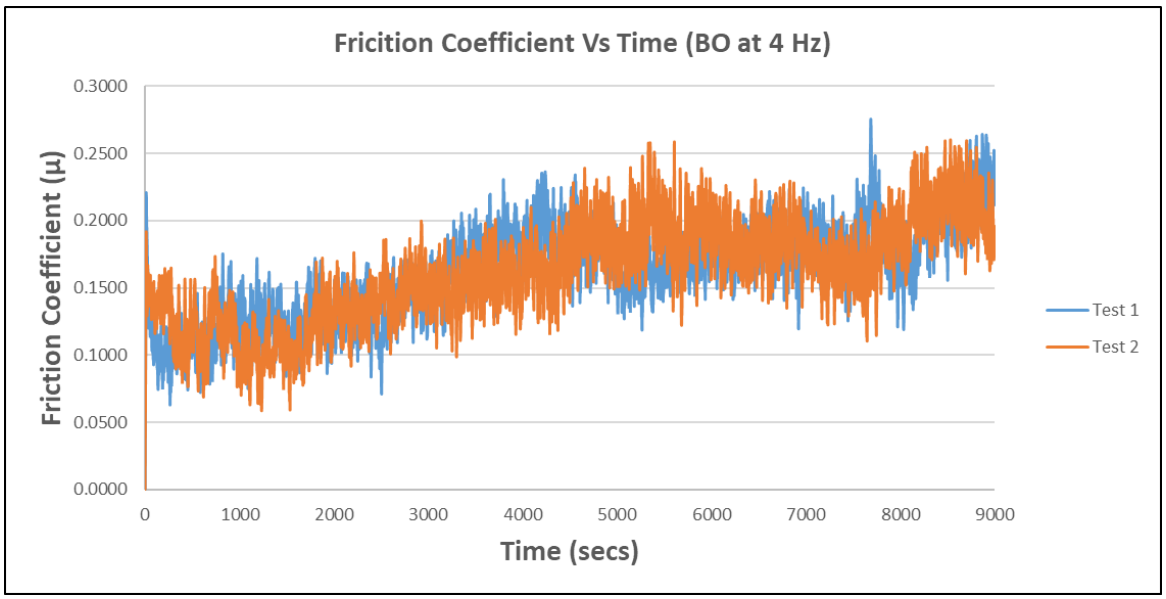

Figure 21: Friction Coefficient Vs Time (BO at 4 Hz).

Figure 22. shows the friction coefficient response with respect to time for all the 3 tests conducted using 1% wt. DCi with BO as neat lubricant at 4 Hz.

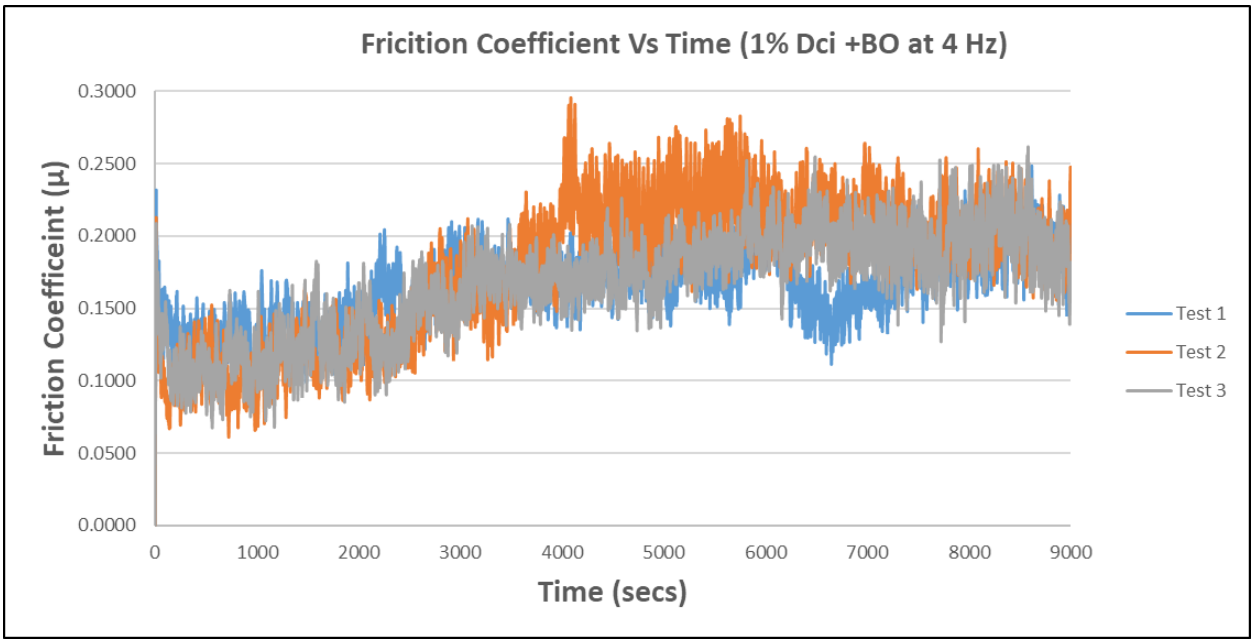

Figure 22: Friction Coefficient Vs Time (1% DCi + BO at 4 Hz).

Figure 23. shows the friction coefficient response with respect to time for all the 3 tests conducted using BO as neat lubricant at 5 Hz.

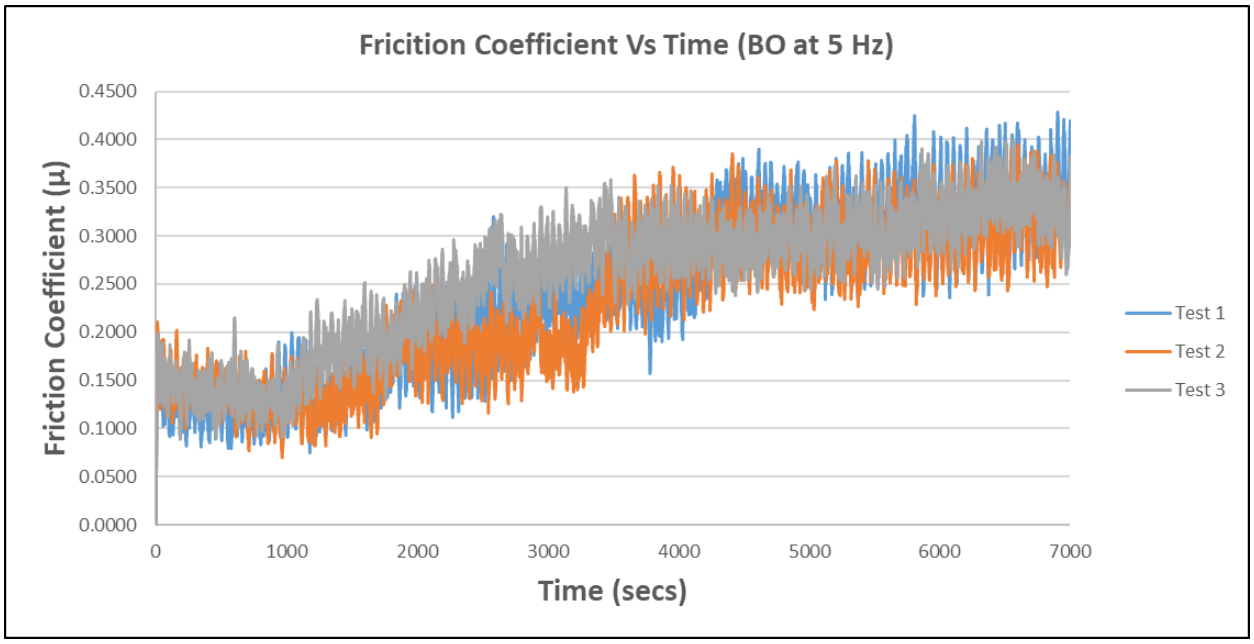

Figure 23: Friction Coefficient Vs Time (BO at 5 Hz).

Figure 24. shows the friction coefficient response with respect to time for both the tests conducted using 1% wt. DCi with BO as neat lubricant at 5 Hz.

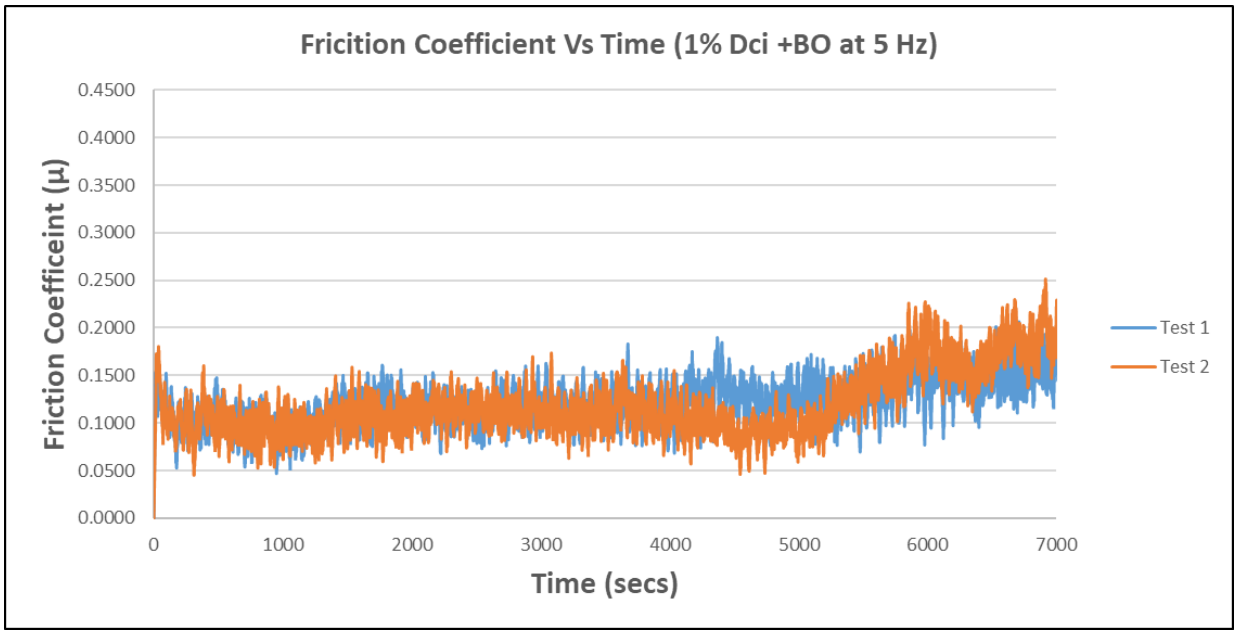

Figure 24: Friction Coefficient Vs Time (1% DCi + BO at 5 Hz).

Moreover, a closer look at Figure 23 and Figure 24, as discussed earlier shows that the sudden jump in the friction coefficient comes at around after 5000 secs while using 1% wt. DCi as an additive to BO as compared to the jump coming after 2000 secs using BO as lubricant. This trend shows the superior lubricating abilities of DCi used as an additive.

7.1.2 Wear – Frequency Based

Wear volume was calculated using equation (2) and (3) with the measured track width. The width of the track was measured using the Olympus B-2 Optical Microscope. Figure 25 shows a sample image captured using the optical microscope while measuring the track width.

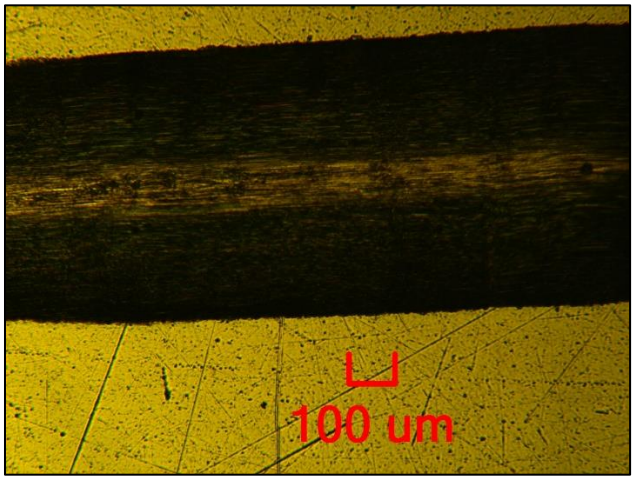

Figure 25: Wear Track Width Measurement Using Olympus B-2.

Table 11 compares the wear volume for all the tests conducted to analyze the tribological performance of both the lubricants used.

Table 9: Comparison of Wear Volume: Frequency Based.

Lubricant	**Frequency**		
	3 Hz	**4 Hz**	**5 Hz**
BO	0.1560 (0.0050)	0.1222 (0.0125)	0.1709 (0.0215)
1% wt. DCi + BO	0.1573 (0.0040)	0.1450 (0.0150)	0.1314 (0.0167)

Figure 26 shows the wear Volume comparison for all the frequency-based tests conducted. It can be clearly seen that the only wear Volume reduction was seen at frequency of 5 Hz which was a great 23% wear Volume reduction.

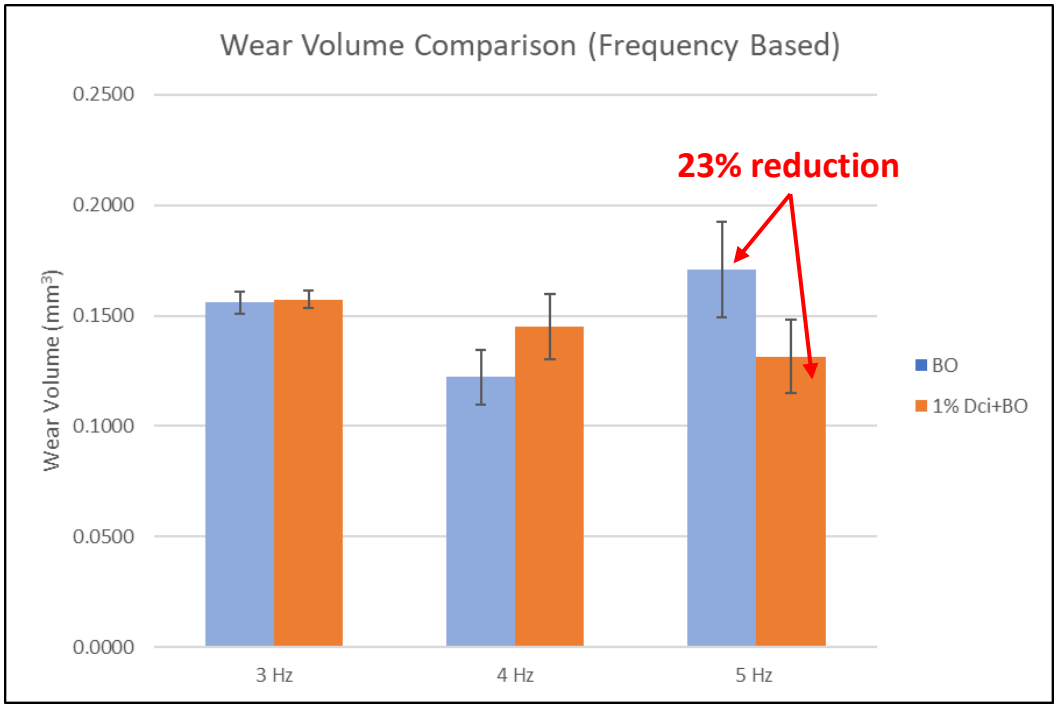

Figure 26: Wear Volume Comparison.

Figure 27 shows the wear rate comparison for all the frequency-based tests conducted. A similar 23% reduction ca be seen at frequency of 5 Hz. Wear rate is calculated as wear Volume over the sliding distance.

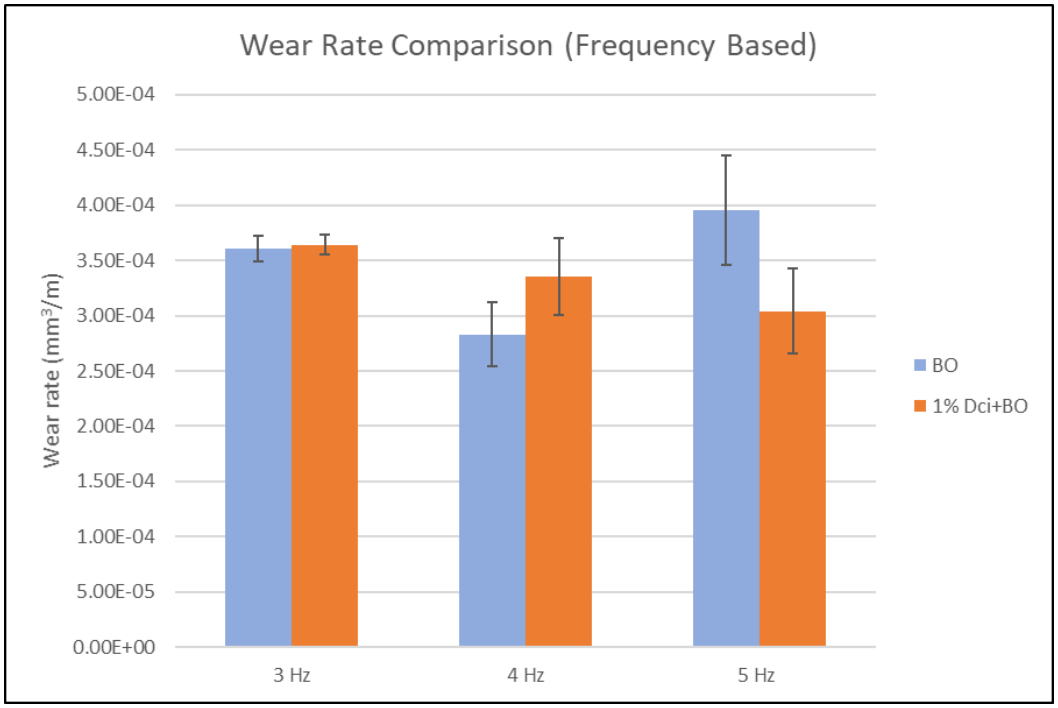

Figure 27: Wear Rate Comparison.

Figure 28 shows the wear rate comparison for all the frequency-based tests conducted. A similar 23% reduction was seen at frequency of 5 Hz. Specific wear rate is calculated by dividing the wear Volume with product of load and sliding distance.

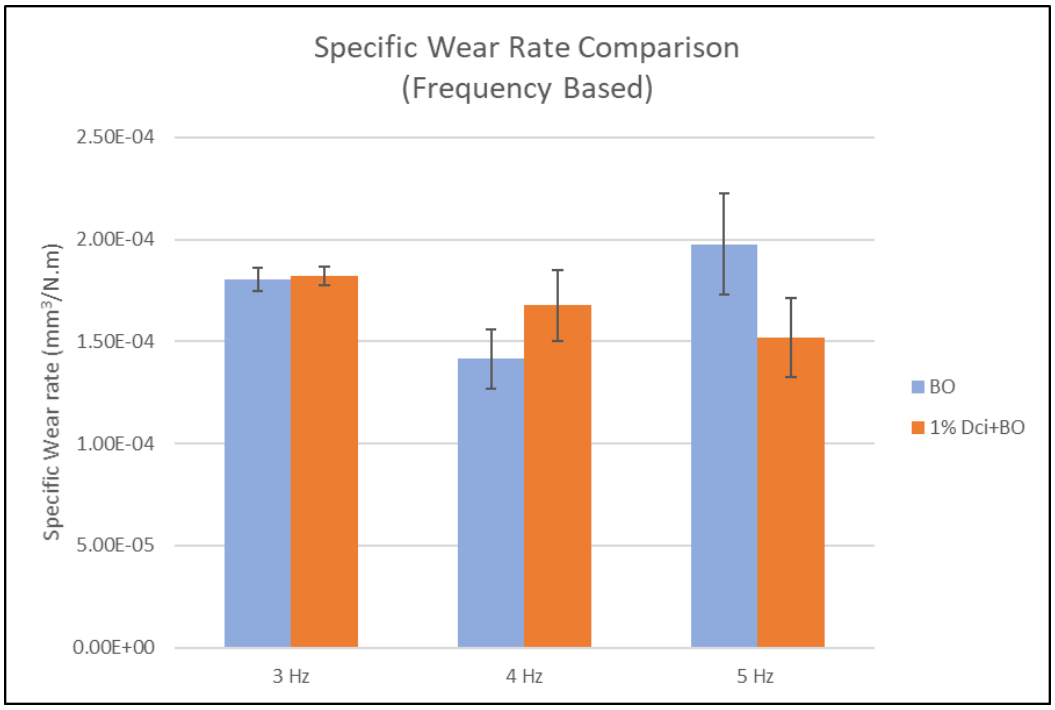

Figure 28: Specific Wear Rate Comparison.

7.2 Load Based Testing

7.2.1 Friction Coefficient

According to the results based on the frequency-based testing, it was clear that the maximum friction reduction was achieved at frequency of 5 Hz. So, it was decided to carry on further testing at frequency of 5 Hz but with different loads. The aim of this testing was to see the variation in friction coefficient with varying loads.

With this additional testing, 21% and 11% friction reduction were seen at load of 1 N and 3 N respectively at a frequency of 5 Hz. Figure 29 summarizes the friction coefficients seen at 1N, 2N and 3N respectively at a frequency of 5 Hz.

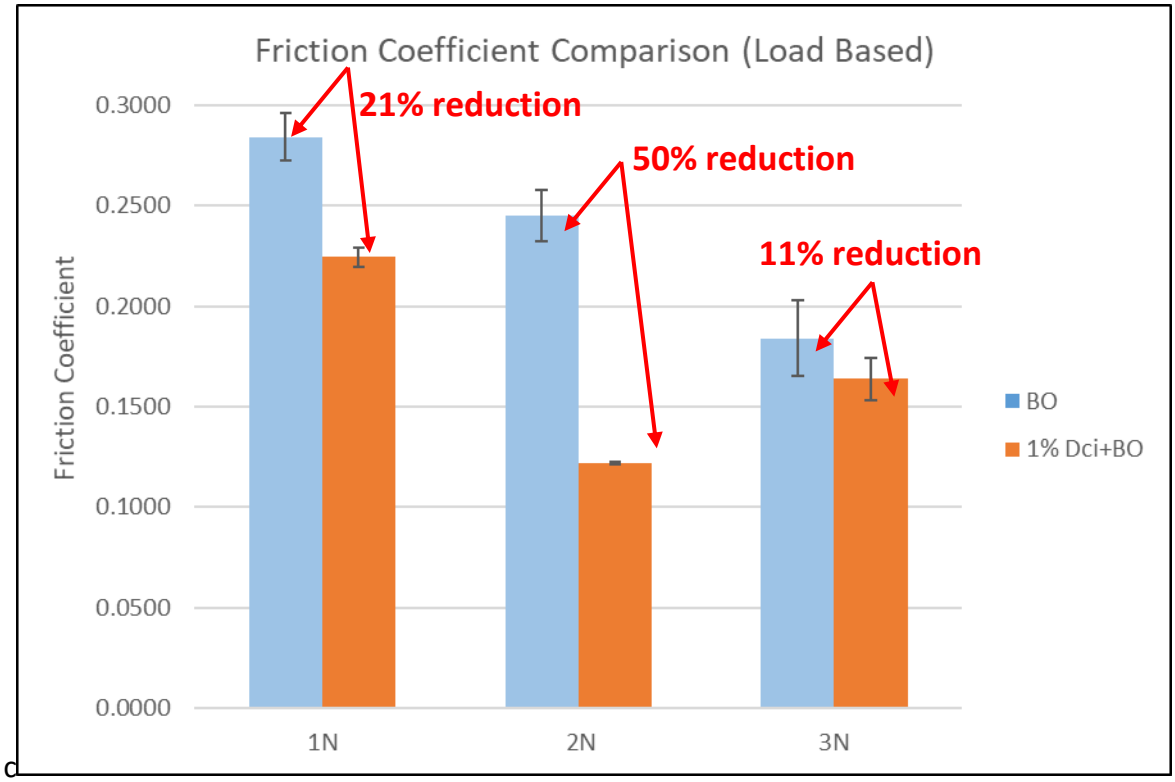

Figure 29: Friction Coefficient Comparison Using BO and 1% DCi + BO.

Table 12. compares the friction coefficient of different tests conducted to compare the tribological performance of these two lubricants.

Table 10: Comparison of Friction Coefficient: Load Based.

Lubricant	Frequency		
	1 N	2 N	3 N
BO	0.2840 (0.011832)	0.2452 (0.012673)	0.1839 (0.01871)
1% wt. DCi + BO	0.2243 (0.004813)	0.1219 (0.000722)	0.1637 (0.010733)

The friction coefficient response with response to time was plotted for all the tests conducted with both lubricants at 3 different loads. Figure 30. shows the friction coefficient response with respect to time for all the 3 tests conducted using BO as neat lubricant at 1N.

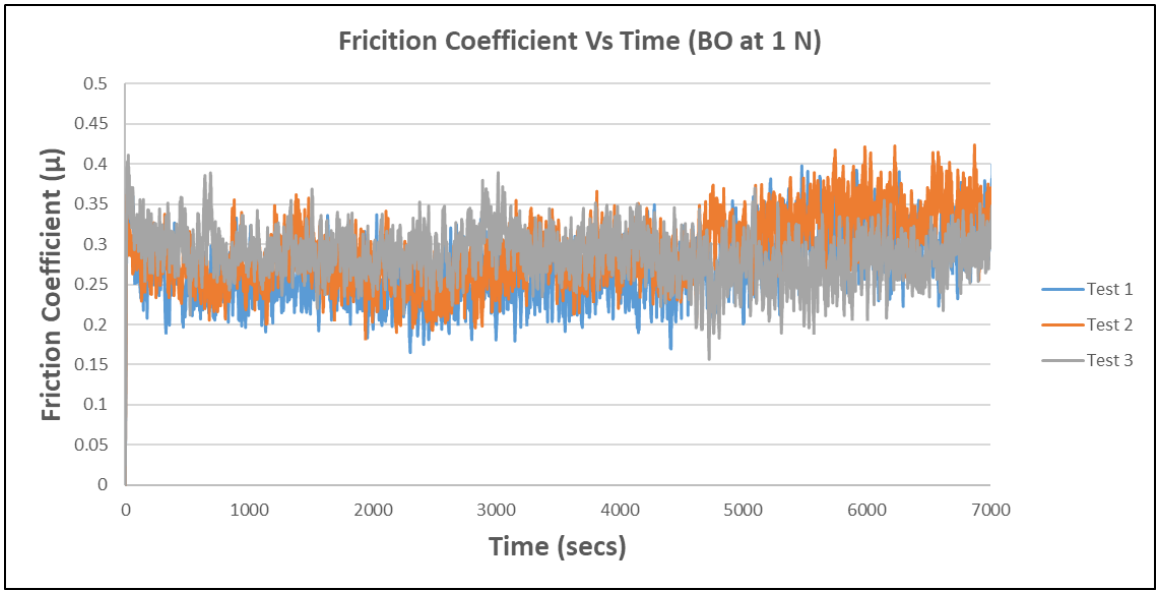

Figure 30: Friction Coefficient Vs Time (BO at 1 N).

Figure 31. shows the friction coefficient response with respect to time for both the tests conducted using 1% wt. DCi with BO as neat lubricant at 1N.

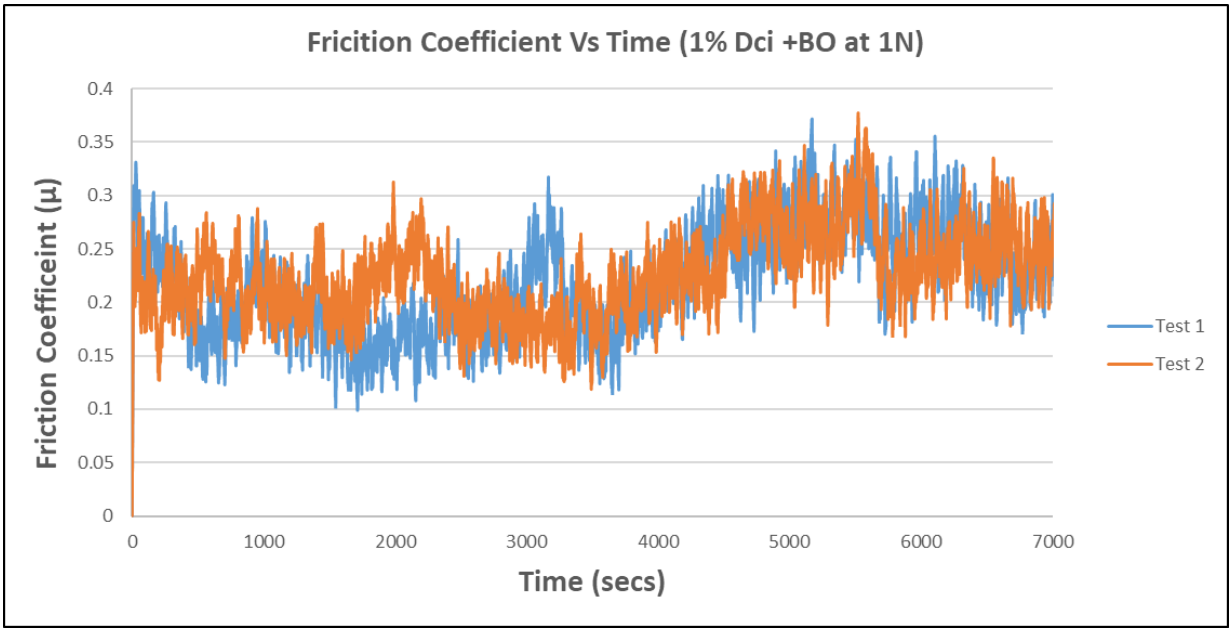

Figure 31: Friction Coefficient Vs Time (1% DCi + BO at 1 N).

The friction coefficient response with respect to time for the tests conducted using BO as neat lubricant and 1% wt. DCi with BO as lubricant can be seen in Figure 23 and Figure 24 respectively.

Figure 32. shows the friction coefficient response with respect to time for both the tests conducted using BO as neat lubricant at 3 N.

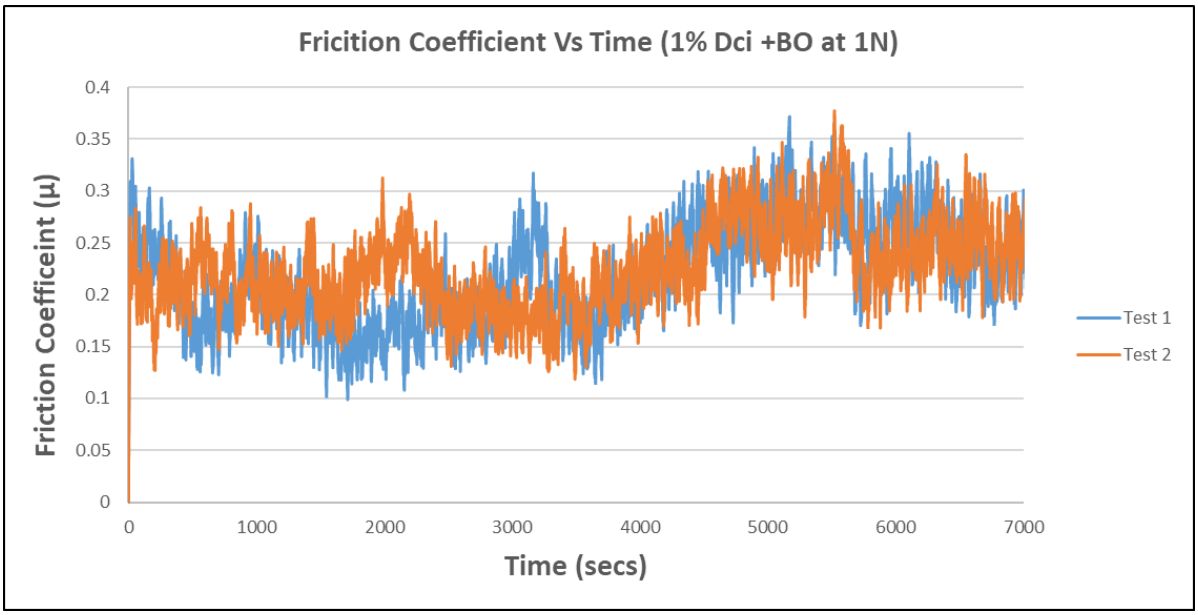

Figure 32: Friction Coefficient Vs Time (BO at 3 N).

Figure 33. shows the friction coefficient response with respect to time for both the tests conducted using 1% wt. DCi with BO as neat lubricant at 3 N.

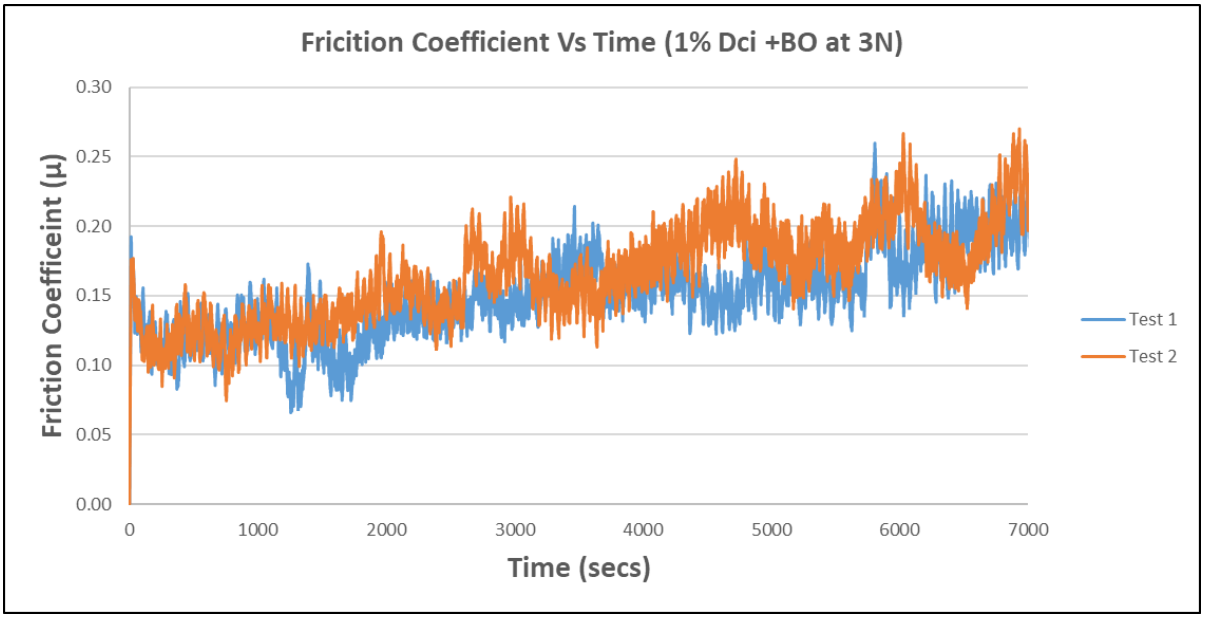

Figure 33: Friction Coefficient Vs Time (1% DCi + BO at 3 N).

7.2.2 Wear – Load Based

Wear Volume was calculated using the track width measured using the Olympus B-2 optical microscope. Table 13 compares the wear Volume for all the tests conducted to analyze the tribological performance of both the lubricants used.

Table 11: Comparison of Wear Volume: Load Based.

Lubricant	**Frequency**		
	1N	**2N**	**3N**
BO	0.0974 (0.0117)	0.1709 (0.0215)	0.2205 (0.019)
1% wt. DCi + BO	0.0906 (0.00943)	0.1314 (0.0167)	0.1592 (0.0075)

Figure 34. shows the wear Volume comparison for all the tests conducted at frequency of 5 Hz and at loads of 1N, 2N and 3N respectively. It can be clearly seen that as the load increases the wear Volume goes on increasing as well. A wear Volume reduction of 7%, 23% and 28% was seen at loads of 1N, 2N and 3N respectively at a frequency of 5 Hz.

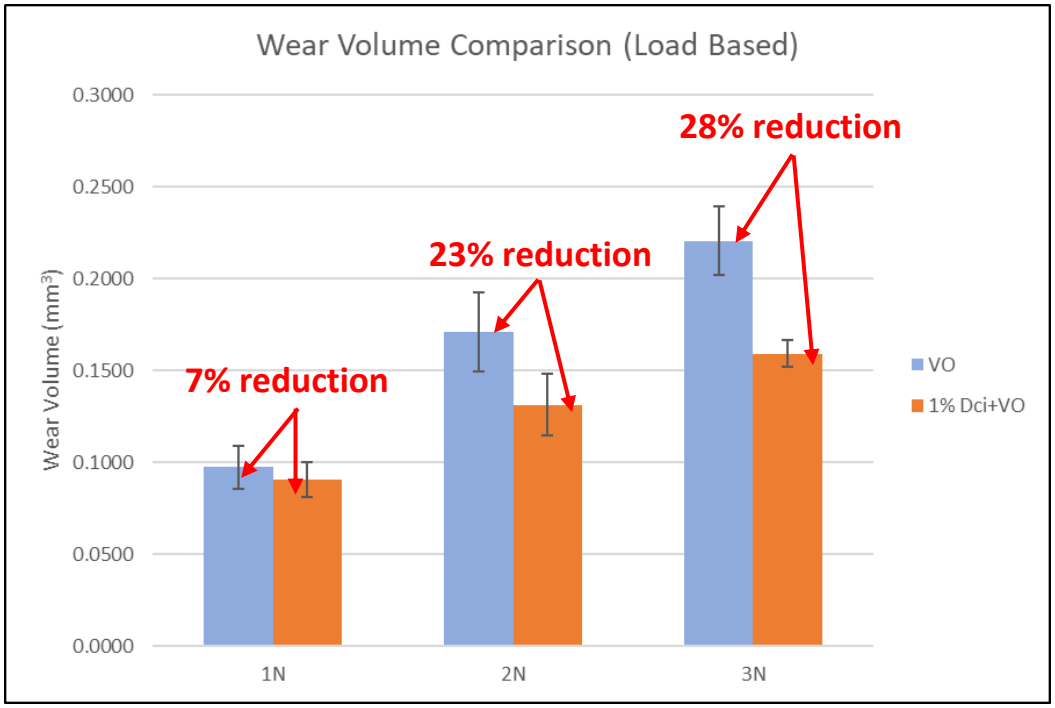

Figure 34: Wear Volume Comparison.

Figure 35 shows the wear rate comparison for all the frequency-based tests conducted. A similar 7%, 23% and 28 % reduction can be seen at loads of 1N, 2N and 3 N respectively. Wear rate is calculated as wear Volume over the sliding distance.

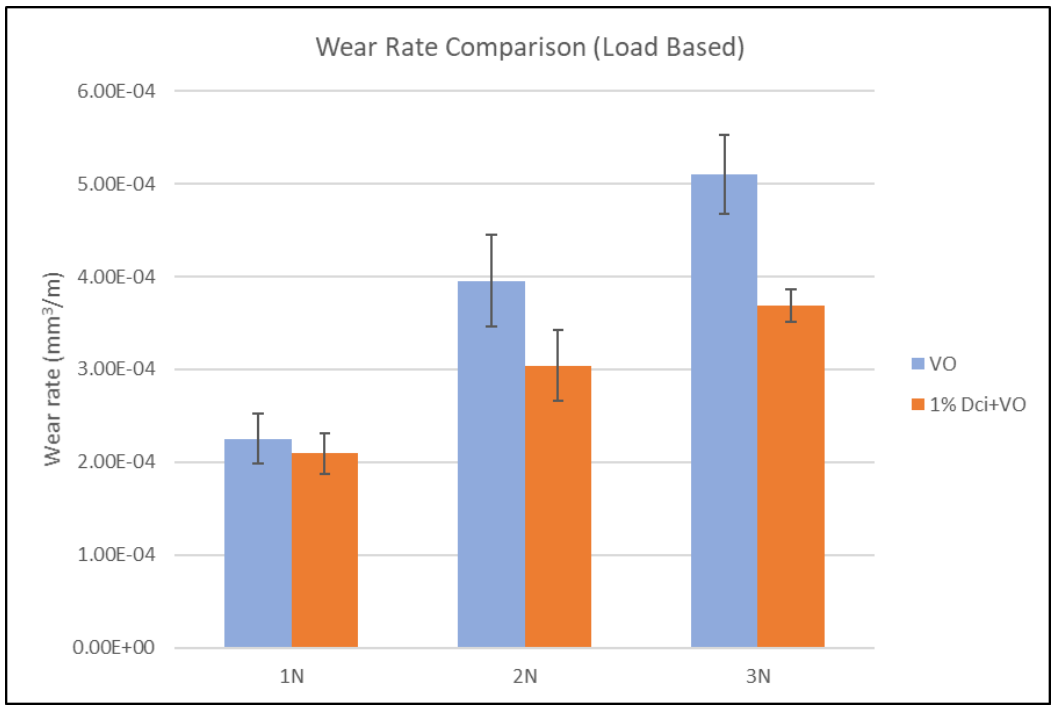

Figure 35: Wear Rate Comparison.

Figure 36 shows the wear rate comparison for all the frequency-based tests conducted. A similar 7%, 23% and 28 % reduction can be seen at loads of 1N, 2N and 3 N respectively. Specific wear rate is calculated by dividing the wear Volume with product of load and sliding distance.

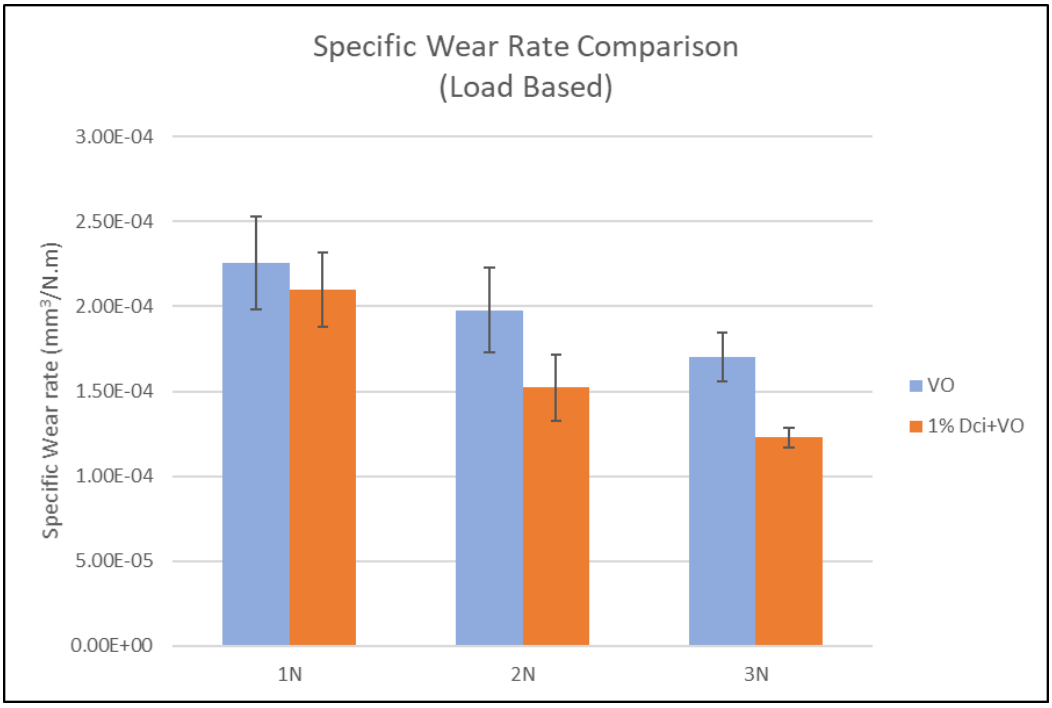

Figure 36: Specific Wear Rate Comparison.

7.3 SEM Analysis

After looking at the friction coefficient and wear Volume calculation it can be clearly seen that the maximum friction reduction of 50% which was the highest amongst all the tests performed and a wear reduction of 23% was seen at frequency of 5 Hz and a load of 2 N. Hence, for further study a TESCAN MIRA 3 SEM (Scanning Electron Microscope) was used to further analyze the wear track obtained by performing tests at above mentioned conditions which resulted in maximum friction reduction.

SEM analysis can be used to get a better idea regarding the type of wear seen on the track. Figure 37 (a) shows the wear track obtained at 5 Hz and 2 N with BO as lubricant as seen under the SEM at 200 x. Figure 36 (b) shows the wear track obtained with 1% wt. DCi with BO as lubricant at frequency of 5 Hz and under load of 2 N.

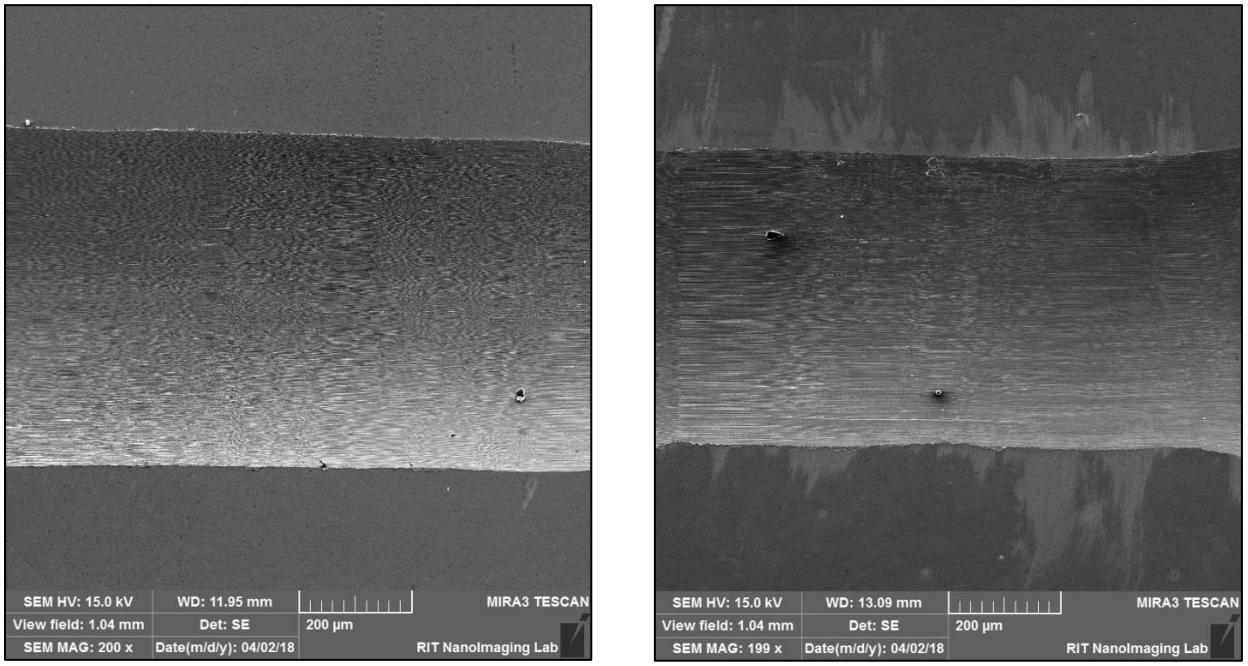

(a). BO at 200 x (b). 1% DCi with BO at 200x

Figure 37: Wear Track as seen under SEM at 200 x.

It can be clearly seen from Figure 36 that the type of wear is abrasive wear for this Ti6Al4V in contact with Tungsten Carbide (WC). Furthermore, to get additional details on abrasive wear marks the wear tracks were studied under higher magnitude.

Figure 38 (a) and (b) show the wear track at frequency of 5 Hz and under load of 2 N while using BO and 1% wt. DCi with BO respectively as lubricants at magnitude of 2000 x.

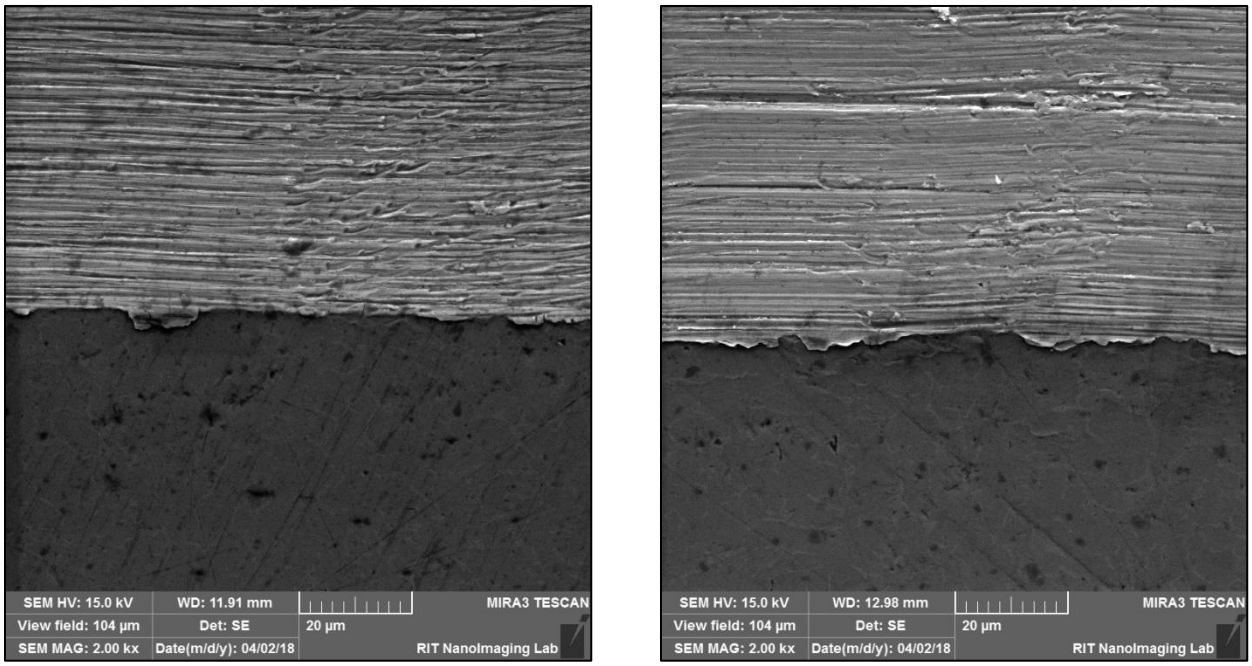

(a). BO at 200 x

(b). 1% DCi with BO at 200x

Figure 38: Wear track as seen under SEM at 2000 x.

As can be seen from Figure 37, the wear track with BO as lubricant seen in Figure 37 (a) shows more abrasion marks as compared to the wear track with 1% wt. DCi with BO as lubricant seen in Figure 37 (b). This clearly, shows the effect of the addition of 1% wt. DCi as an additive to Bio Telex 46 (BO) used as the base oil.

7.4 EDX Analysis

The type of wear was identified using the SEM analysis. Using the same SEM an Energy Dispersive X-Ray (EDX) analysis was performed to identify the elements present on the disk sample. This will give us idea regarding material deposition and also the interaction between the metals in contact with each other.

Figure 39 shows the comparison of BO against 1% DCi with BO used at lubricant inside the wear track.

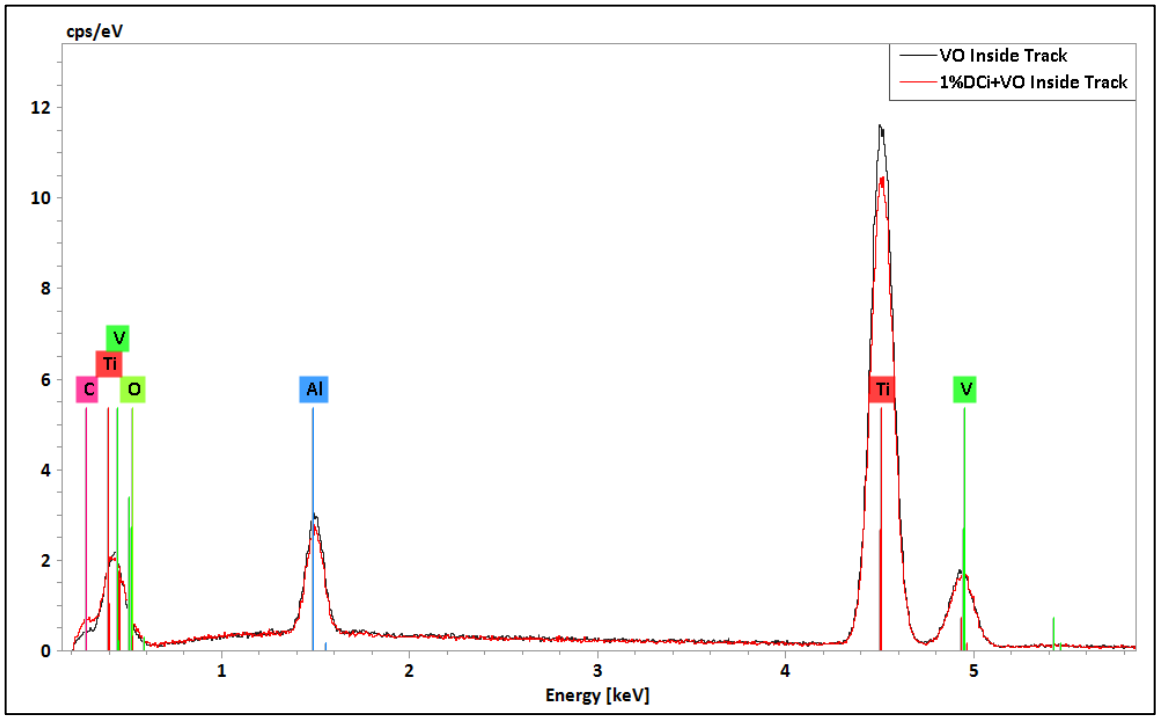

Figure 39: Comparison of BO Vs 1% DCi Inside the Wear Track at 5Hz; 2 N.

As can be seen from Figure 38, more carbon can be seen inside the wear track with 1% DCi as lubricant as compared to BO as lubricant. This carbon deposit is from the rich tribolayer formed due to the IL.

Figure 40 shows the comparison of BO against 1% DCi with BO used as lubricant outside of the wear track. No significant difference between BO and 1% DCi with BO used as lubricant can be seen outside the wear track.

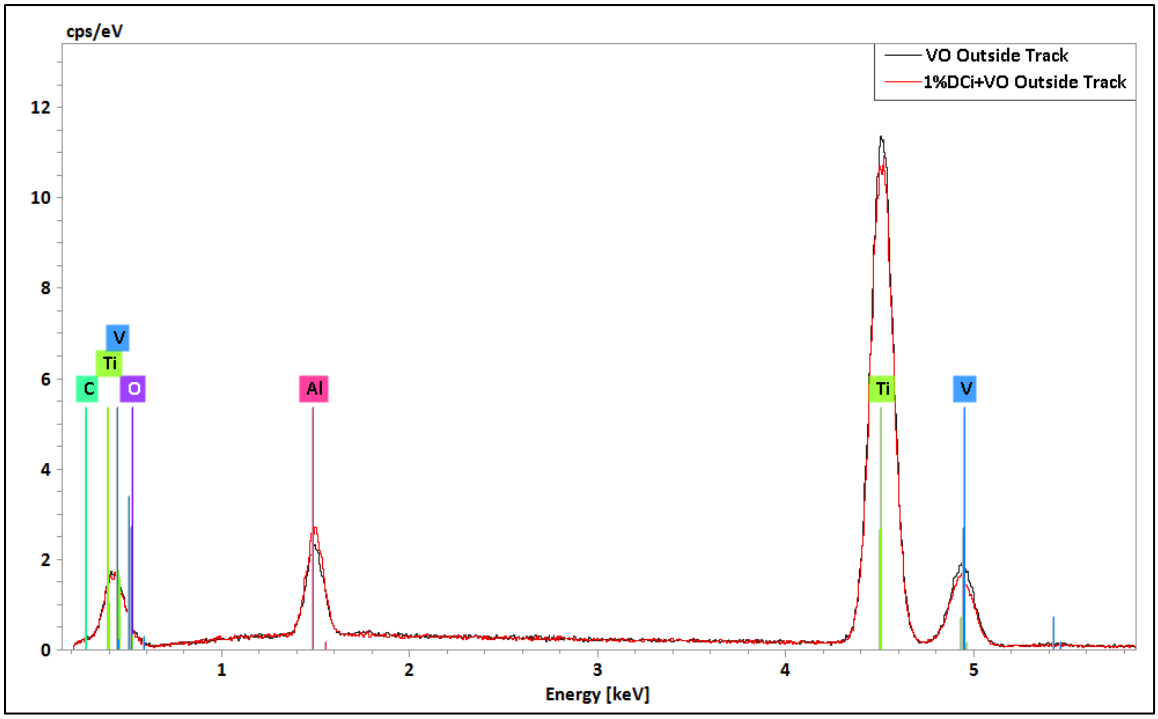

Figure 40: Comparison of BO Vs 1% DCi Outside the Wear Track at 5Hz; 2 N.

A very small difference in the amount of Titanium (Ti), Vanadium (V) and Aluminum (Al) can also be seen with the use of 1% DCi as an additive into BO.

8.0 CONCLUSION

Tri-[bis(2-hydroxyethylammonium)] Citrate (DCi), a halogen-free IL synthesized at RIT was used as 1% wt. additive to Bio Telex 46 which is a biodegradable oil and its effect on friction and wear reduction in Titanium-Ceramic contact was studied in this research. Frequency and load were the parameters which were varied in this study. The conclusion from the results of this research can be given as follows:

1. The addition of 1% wt. DCi as an additive to Bio Telex 46 used as lubricant showed significant reduction of friction coefficient and wear Volume as compared to that of Bio Telex 46 (BO) being used as lubricant.
2. The frequency-based testing resulted in almost no friction coefficient reduction at 3 Hz and 4 Hz but achieved the maximum 50% friction coefficient reduction at 5 Hz. A similar trend was seen in terms of wear Volume reduction, where a maximum 23% reduction was seen at 5 Hz and almost no wear reduction was seen at 3 Hz and 4 Hz.
3. The load-based testing which was conducted looking at the frequency-based testing results, showed a maximum 23% friction coefficient at 2N and also, a 21% and 11% friction coefficient reduction at 1N and 3N respectively.
4. However, with the load-based testing, unlike the friction coefficient, the wear Volume reduction seemed to be increasing with the increasing load. A reduction of 7%, 23% and the maximum 28% was seen at loads of 1N, 2N and 3N respectively.

9.0 SOCIETAL CONTEXT

Ionic Liquids have a great potential of decreasing the friction and wear between any bodies in contact with each other. Decreasing the wear Volume can increase the life of any component thus in return reducing the servicing and operating cost of the component. Protic ionic liquids have a lot of advantages over aprotic ionic liquids like lower cost and ease to synthesize. They also have a wide range of applications like chromatography, protein synthesis, antimicrobial, bacterial endospore detection [22].

As compared to APILs vast amount of literature availability, there have been very few publications on PIL, given the fact that they can be used for a variety of same applications as the APILs like use in chromatography, organic synthesis, as amphibole self-assembly media, electrochemistry, as explosives, as well as in additional applications where an available proton is essential for many biomedical applications and also as proton-conducting media for polymer membrane fuel cells [22].

Titanium has a lot of potential to be used as reliable material with high strength, corrosion resistance and high load bearing capacity. The cost reduction for titanium is possible by reducing the machining cost of titanium. After that it can be used in the biomedical industry, construction and automotive industry.

Titanium can be used in the biomedical industry for artificial hip joints, artificial knee joints, bone plates, screws for fracture fixation, cardiac valve prostheses, pacemakers and artificial hearts. It can also be used for dentistry devices such as implants, crowns, bridges, overdentures etc. The material properties that are responsible for biocompatibility are low level of electronic

conductivity, high corrosion resistance, low ion-formation tendency in aqueous environment and electronic point of oxide of 5-6 [34].

Modern building constructions can use titanium sheets for protection of the building from corrosion. A system to compensate for thermal expansion and contraction are required for large roofs made of thin titanium sheets. Titanium sheets can be made from single panels as the thermal stress is less than compared to other materials like steel, copper and aluminum [35].

Titanium has very wide variety of application in the automotive industry due to its properties like high strength to weight ratio that can reduce weight in body, frame and suspension, excellent temperature resistance properties coupled with its light weight and corrosion resistance makes it attractive for engine components. It can also be used in the exhaust system due to excellent thermal resistance and corrosion resistance. Even the high cost can be offset by the savings in fuel economy and improvements in handling due to weight reduction [36].

All the above-mentioned advantages of titanium can be made feasible with the use of protic ionic liquids without damaging or polluting the environment.

10.0 FUTURE RESEARCH

Even the results from this research demonstrated great friction and wear reduction, there are a few areas in which this research can be carried on forward. These areas are as follows:

- Different halogen-free IL's can be studied to see the impact of change of IL on the friction and wear reduction. The chemical interaction as a result of using a different IL as a lubricant can further give us an idea regarding the use of halogen-free ionic liquids as an additive to lubricants.
- While 1% wt. DCi was used as an additive for this research, different concentrations of DCi can be tried and their impact on friction and wear reduction can be studied. Also, it might impact the type of wear on the sample disk.
- The sliding distance was a constant in this research. The possibility of varying the sliding distance and studying its effect can also be a potential way forward.

11.0 APPENDIX

Annex A: MATLAB code for wear Volume

```
% Program to calculate the wear volume of sliders with non-flat wear scars.
clear all
clc

% terms used
% Vf= wear volume; Ls= Stroke Length; W= track width; Rf= radius of ball
% To calulate hf in mm
Rf = 0.75;
W1 = 638.487;
W = 0.001*W1; % convert track width from micrometers to mm
hf = Rf -sqrt((Rf^2)-((W^2)/4)) %to calculate wear depth in mm

% To calculate wear volume in mm^3
Ls = 6;
Vf = (Ls*(((Rf^2)*asind(W/(2*Rf)))-((W/2)*(Rf-hf))))+((pi/3)*((hf^2)))*((3*Rf)-hf)
```

12.0 REFERENCES

[1] Cupillard, S., 2007, “Lubrication of Conformal Contacts with Surface Texturing,” p. 98.

[2] Revuru, R. S., Posinasetti, N. R., Vsn, V. R., and Amrita, M., 2017, “Application of Cutting Fluids in Machining of Titanium Alloys—a Review,” Int. J. Adv. Manuf. Technol., **91**(5–8), pp. 2477–2498.

[3] Zhou, F., Liang, Y., and Liu, W., 2009, “Ionic Liquid Lubricants: Designed Chemistry for Engineering Applications,” Chem. Soc. Rev., **38**(9), p. 2590.

[4] Cigno, E., Magagnoli, C., Pierce, M. S., and Iglesias, P., 2017, “Lubricating Ability of Two Phosphonium-Based Ionic Liquids as Additives of a Bio-Oil for Use in Wind Turbines Gearboxes,” Wear, **376**–**377**, pp. 756–765.

[5] Grace, J., Vysochanska, S., Lodge, J., and Iglesias, P., 2015, “Ionic Liquids as Additives of Coffee Bean Oil in Steel-Steel Contacts,” Lubricants, pp. 637–649.

[6] Gutierrez, M., Haselkorn, M., and Iglesias, P., 2016, “The Lubrication Ability of Ionic Liquids as Additives for Wind Turbine Gearboxes Oils,” Lubricants, **4**(2), p. 14.

[7] Minami, I., 2009, “Ionic Liquids in Tribology.,” Molecules, **14**(6), pp. 2286–2305.

[8] Bermudez, M. D., Jimenez, A. E., Sanes, J., and Carrion, F. J., 2009, “Ionic Liquids as Advanced Lubricant Fluids,” Molecules, **14**(8), pp. 2888–2908.

[9] Totolin, V., Minami, I., Gabler, C., and Dorr, N., 2013, “Halogen-Free Borate Ionic Liquids as Novel Lubricants for Tribological Applications,” Tribol. Int., **67**, pp. 191–198.

[10] Goindi, G. S., Chavan, S. N., Mandal, D., Sarkar, P., and Jayal, A. D., 2014, "Investigation of Ionic Liquids As Metalworking Fluids in Minimum Quantity Lubrication Machining of Aisi 1045 Steel," (Aimtdr), pp. 3–8.

[11] Goindi, G. S., Sarkar, P., Jayal, A. D., Chavan, S. N., and Mandal, D., 2017, "Investigation of Ionic Liquids as Additives to Canola Oil in Minimum Quantity Lubrication Milling of Plain Medium Carbon Steel," Int. J. Adv. Manuf. Technol., pp. 1–16.

[12] Goindi, G. S., Chavan, S. N., Mandal, D., Sarkar, P., and Jayal, A. D., 2015, "Investigation of Ionic Liquids as Novel Metalworking Fluids during Minimum Quantity Lubrication Machining of a Plain Carbon Steel," Procedia CIRP, **26**, pp. 341–345.

[13] Davis, B., Schueller, J. K., and Huang, Y., 2015, "Study of Ionic Liquid as Effective Additive for Minimum Quantity Lubrication during Titanium Machining," Manuf. Lett., **5**, pp. 1–6.

[14] Jiménez, A. E., and Bermúdez, M. D., 2009, "Ionic Liquids as Lubricants of Titanium-Steel Contact," Tribol. Lett., **33**(2), pp. 111–126.

[15] Mobarak, H. M., Niza Mohamad, E., Masjuki, H. H., Kalam, M. A., Al Mahmud, K. A. H., Habibullah, M., and Ashraful, A. M., 2014, "The Prospects of Biolubricants as Alternatives in Automotive Applications," Renew. Sustain. Energy Rev., **33**, pp. 34–43.

[16] Pramanik, A., and Littlefair, G., 2015, "Machining of Titanium Alloy *(Ti-6Al-4V)* —Theory to Application," Mach. Sci. Technol., **19**(1), pp. 1–49.

[17] Bhushan, B., *Introduction to Tribology*.

[18] David Doyle, "Lubrication Starvation."

[19] Mehta, P., 2016, “Tribological Study of Textured Surfaces Created Using Modulation Assisted Machining for Steel- Aluminum Contact.”

[20] Cigno, E., 2016, “Tribological Study of High Performance Bio- Lubricants Enhanced with Ionic Liquids for Use in Wind Turbines.”

[21] Bossung, K., 2017, “IMECE2016-66048 EFFECT OF HALOGEN-FREE IONIC LIQUIDS AS ADDITIVIES OF BIOLUBRICANTS FOR ROOM TEMPERATURE TITANIUM-STEEL CONTACT,” pp. 1–6.

[22] Greaves, T. L., and Drummond, C. J., 2008, “Protic Ionic Liquids: Properties and Applications,” Chem. Rev., **108**(1), pp. 206–237.

[23] Patel, A., Guo, H., and Iglesias, P., 2018, “Study of the Lubricating Ability of Protic Ionic Liquid on an Aluminum–Steel Contact,” Lubricants, **6**(3), p. 66.

[24] Khan, M. M. A., Mithu, M. A. H., and Dhar, N. R., 2009, “Effects of Minimum Quantity Lubrication on Turning AISI 9310 Alloy Steel Using Vegetable Oil-Based Cutting Fluid,” J. Mater. Process. Technol., **209**(15–16), pp. 5573–5583.

[25] Srikant, R. R., Prasad, M. M. S., Amrita, M., Sitaramaraju, A. V., and Krishna, P. V., 2014, “Nanofluids as a Potential Solution for Minimum Quantity Lubrication: A Review,” Proc. Inst. Mech. Eng. Part B J. Eng. Manuf., **228**(1), pp. 3–20.

[26] Boubekri, N., and Shaikh, V., 2014, “Minimum Quantity Lubrication (MQL) in Machining: Benefits and Drawbacks,” J. Ind. Intell. Inf., **3**(3), pp. 205–209.

[27] Kurgin, S., Dasch, J. M., Simon, D. L., Barber, G. C., and Zou, Q., 2014, “A Comparison of

Two Minimum Quantity Lubrication Delivery Systems," Ind. Lubr. Tribol., **66**(1), pp. 151–159.

[28] Nath, C., Kapoor, S. G., Srivastava, A. K., and Iverson, J., 2013, "Effect of Fluid Concentration in Titanium Machining with an Atomization-Based Cutting Fluid (ACF) Spray System," J. Manuf. Process., **15**(4), pp. 419–425.

[29] Atomization, A. N., Cutting, B., Acf, F., System, S., Hoyne, A. C., and Nath, C., 2014, "Imece2013-63898 Cutting Temperature Measurement During Titanium Machining With."

[30] Guo, H., Iglesias Victoria, P., Fuentes Aznar, A., and Liu, R., 2017, "FRICTION AND WEAR PROPERTIES OF HALOGEN-FREE AND HALOGEN- CONTAINING IONIC LIQUIDS USED AS NEAT LUBRICANTS, LUBRICANT ADDITIVES AND THIN LUBRICANT LAYERS," Int. Des. Eng. Tech. Conf. Comput. Inf. Eng. Conf., pp. 1–6.

[31] Qu, J., and Truhan, J. J., 2006, "An Efficient Method for Accurately Determining Wear Volumes of Sliders with Non-Flat Wear Scars and Compound Curvatures," Wear, **261**(7–8), pp. 848–855.

[32] "Biotelex 46 Lubriant Properties: Https://Www.Repsol.Com/Imagenes/Global/En/RP_BIO_TELEX_EN_tcm14-62571.Pdf."

[33] Heerwan, M., and Peeie, B., "BMA4723 VEHICLE DYNAMICS Ch3 Tire Mechanics By."

[34] Elias, C. N., Lima, J. H. C., Valiev, R., and Meyers, M. A., 2008, "Biomedical Applications of Titanium and Its Alloys," J. Miner. Met. Mater. Soc., (March), pp. 46–49.

[35] Adamus, J., 2014, "Applications of Titanium Sheets in Modern Building Construction," Adv.

Mater. Res., **1020**, pp. 9–14.

[36] Sherman, A. ., and Allison, J. ., “Potential for Automotive Applications of Titanium Alloys.”